Fall 2016

Mitigation of wellbore instability in deviated wells by using geomechanical models and MPD technique

Husam Raad Abbood

Department:

MITIGATION OF WELLBORE INSTABILITY IN DEVIATED WELLS BY USING GEOMECHANICAL MODELS AND MPD TECHNIQUE

by

HUSAM RAAD ABBOOD

A THESIS

Presented to the Faculty of the Graduate School of the

MISSOURI UNIVERSITY OF SCIENCE AND TECHNOLOGY

In Partial Fulfillment of the Requirements for the Degree

MASTER OF SCIENCE IN PETROLEUM ENGINEERING

2016

Approved by

Ralph Flori, Advisor
Peyman Heidari
Steven Hilgedick

PUBLICATION THESIS OPTION

This thesis consists of the following two articles, formatted in the style utilized by Missouri University of Science and Technology. Paper I, comprising pages 8 through 50, is submitted to The Journal of Rock mechanic and Geotechnical Engineering, under the tittle ‘‘Case Study of Wellbore Stability Evaluation for the Mishrif Formation, Iraq’’. Paper II, comprising pages 51 through 71, is submitted as a conference paper to the Society of Petroleum Engineering under the title ‘‘A New Driver for Managed Pressure Drilling: Reducing Stuck Pipe Occurrence”.

ABSTRACT

During drilling operations for the E oilfield in the Mishrif formation in southern Iraq, stuck pipe presents a significant wellbore stability problem for deviated wells. In this study, two solutions are utilized to address this problem. The first approach is a 1-D Geomechanical model of the Mishrif formation compiled based on the state of stress and rock strength parameters. It is utilized to assess the contribution of borehole collapse leading to the stuck pipe problems. The results of this study show that wells characterized by stuck pipe are drilled along azimuths which promote wellbore collapse. Three different failure criteria, the Mohr-Coulomb, Mogi-Coulomb, and Modified Lade rock failure criteria, are investigated to determine feasible drilling trajectories and mud pressure conditions for many different wells in the Mishrif Formation. If a specific azimuth for a well cannot be altered, an optimum inclination is recommended to reduce the severity of the borehole collapse. However, the optimum drilling inclination progressively changes as the intermediate principal in-situ stress increases. The second approach is evaluating the feasibility of using the managed pressure drilling (MPD) to optimize the drilling process by controlling mud weight while applying required surface pressure to achieve the target bottom hole pressure (BHP). DZxION CSM software simulation uses different mud weights to determine required choke surface backpressure (SBP) to achieve the initial target equivalent circulation density (ECD). This study discusses hydraulic simulation software used to model the drilling development plan. The software optimizes MPD parameters and discusses the sensitivity effects of each parameter on wellbore pressure and provides guidelines for managing pressure by adjusting these variables.

ACKNOWLEDGMENTS

I would like to express my sincere gratitude to all members of the Higher Committee of Education Development in Iraq for rewarding me full funded scholarship and for their friendly assistance throughout the study.

I would like to gratefully thank my advisor, Dr. Ralph E. Flori for approving me to join his research group. His encouragement, inspiration, and critical comments and correction of the thesis made this work possible.

I would like to thank my defense committee members, Dr. Peyman Heidari and Dr. Steven Hilgedick for their time and efforts in examining the thesis and all the constructive feedbacks.

Dr. Andreas Eckert is gratefully acknowledged for helping me in the Geomechanical part in this research.

Special thanks are due to Dr. Sagar Nauduri and Mr. George Medley for kindly providing me the CSM software and sharing information with me.

I also want to thank the Ikon science company for providing me the RockDoc software and their great technical support.

I would to acknowledge my research group member Ethar Alkamil for his help and valuable discussions.

I want to express my sincere gratitude to the members of Engineering Research Laboratory (ERL). Especially, Ms. Frieda Adams for her support and friendship.

Last but not least, a great thanks to my family. Words cannot express how grateful I am to them for all the supports and encouragements.

TABLE OF CONTENTS

Page

LIST OF FIGURES

LIST OF TABLES

SECTION

1. INTRODUCTION

The E oil-field is a super-giant field located in southern Iraq which covers approximately 900 km2 area with an estimated 38 billion bbls STOIIP (stock tank oil in place) in multiple reservoirs.

The field is currently in the first stages of commercial plan development, field assessment, and reservoir characterization. Based on the data obtained from the vertical wildcat wells, several deviated wells have been drilled for long-term production. The majority of those deviated wells experienced severe wellbore-stability issues in the drilling and completion stages, while only a few were completed without any wellbore-stability issues. The field owner and operator companies did not have a consistent agreement between the recommended mud weight (MW) and the field observations. The reason for the difference between the actual MW and recommended one could be interpreted as follows:

- Lack of provided data
- Time restriction
- Lack of geological knowledge for this area.

Later, a few deviated sidetrack wells were drilled with severe wellbore-stability issues. The drilling progress charts for one of these wells are illustrated in Figure 1.1. Stuck pipe, unplanned sidetracks, incomplete well-logging data collection as well as completing the

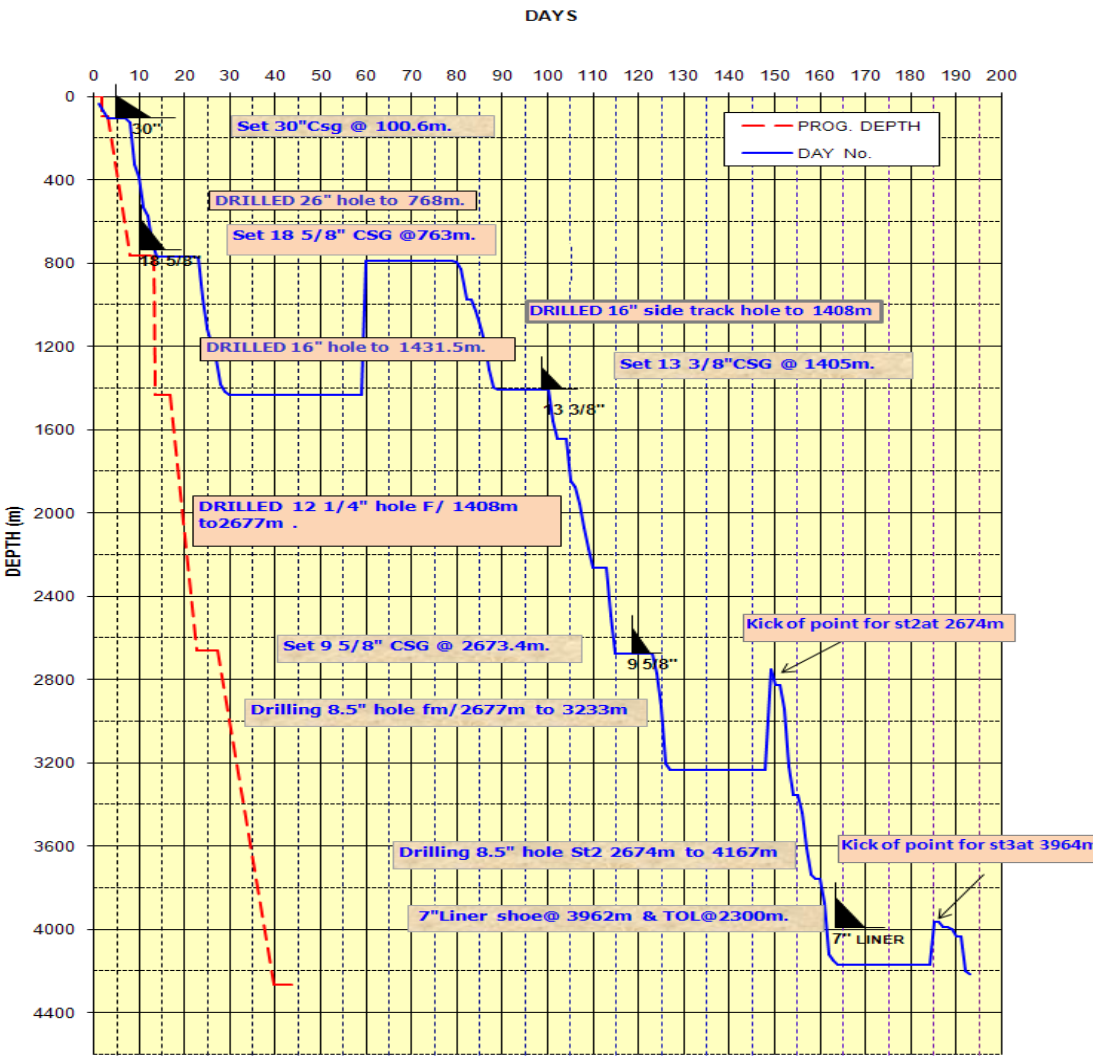

Figure 1.1: The drilling progress chart

problematic deviated sidetrack wells. Figure 1.1 shows that the deviation between planned (dashed red line) and actual curve (blue line) occurs especially in the Mishrif reservoir. Analysis of the well problems indicates the feasibility of reducing or even avoiding wellbore instability problems with manipulating mud weight (MW). First, however, the exact collapse pressure should be constrained. Therefore, a rigorous wellbore-stability analysis needed to be conducted.

1.1 OBJECTIVES OF THE STUDY

The purpose of this study is to determine the required drilling fluid density and to optimize the well trajectory for future drilling operations and field development. This has been done using an integrated wellbore stability analysis in conjunction with the offset-well data. After the input data acquisition, the stress regime in the E oil-field was identified as the normal regime. The obtained input data was used in the new geomechanical model which is based on the conventional rock stress alteration (Kirsch) near the wellbore due to the placement of an arbitrarily inclined well.

The derived wellbore stability model was calibrated using the drilling information, logging data and geological model. A history match of the observed field wellbore-stability cases with the coupled model was obtained. Then, the drilling programs for future wells in the study field were enhanced by designing optimized mud programs for any given wellbore trajectory. Based on the outcomes of this study, recommendations for the future field development have been provided.

In addition, this study investigates using the new leading technology, either under balance drilling (UBD) or managed pressure drilling (MPD), to optimize the drilling process by using the reasonable mud weight and adjusted bottom-hole pressure by applying pressure to the surface to keep the well stable.

1.2 GEOLOGIC FEATURES

The E oil-field s is a double-plunging symmetrical anticline about 60 km long and 15 km wide, with closure in the order of 400 meters for the middle and early Cretaceous reservoirs. Thirteen separate hydrocarbon-bearing horizons have been identified in

carbonate and clastic reservoirs, including Miocene (Ghar formation), late Cretaceous (Shiranish, Hartha, Saadi, Tanuma and Khasib formations) and early Cretaceous (Mishrif, Ahmadi, Nahr Umr, Shuaiba, Yamama and Zubair formations). The source rocks for the field are thought to be the Middle Jurassic shale of the Sargelu and Naokelekan formations(Aqrawi et al., 2005, Jassim and Goff, 2006).

Several regional unconformities and shales provide seals for the oil pools, with Nahr Umr shale being a particular effective seal horizon for major accumulations. The stratigraphic column of the E oilfield is illustrated in Figure 1.2, and the geological prognosis is based on the most recent mapping of the field structure illustrated in Figure 1.3.

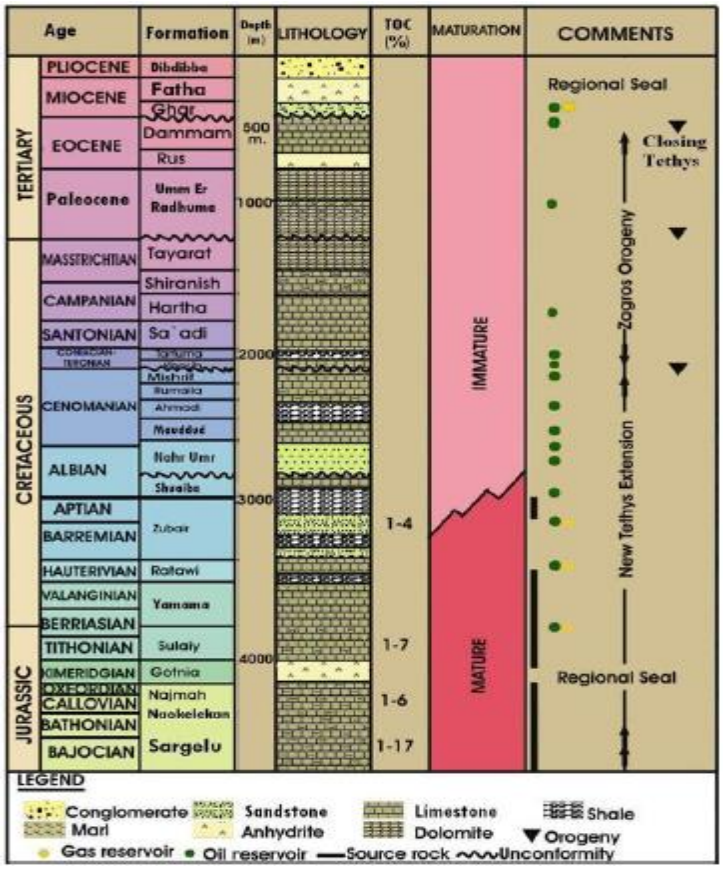

Figure 1.2: The stratigraphic column of the E oilfield

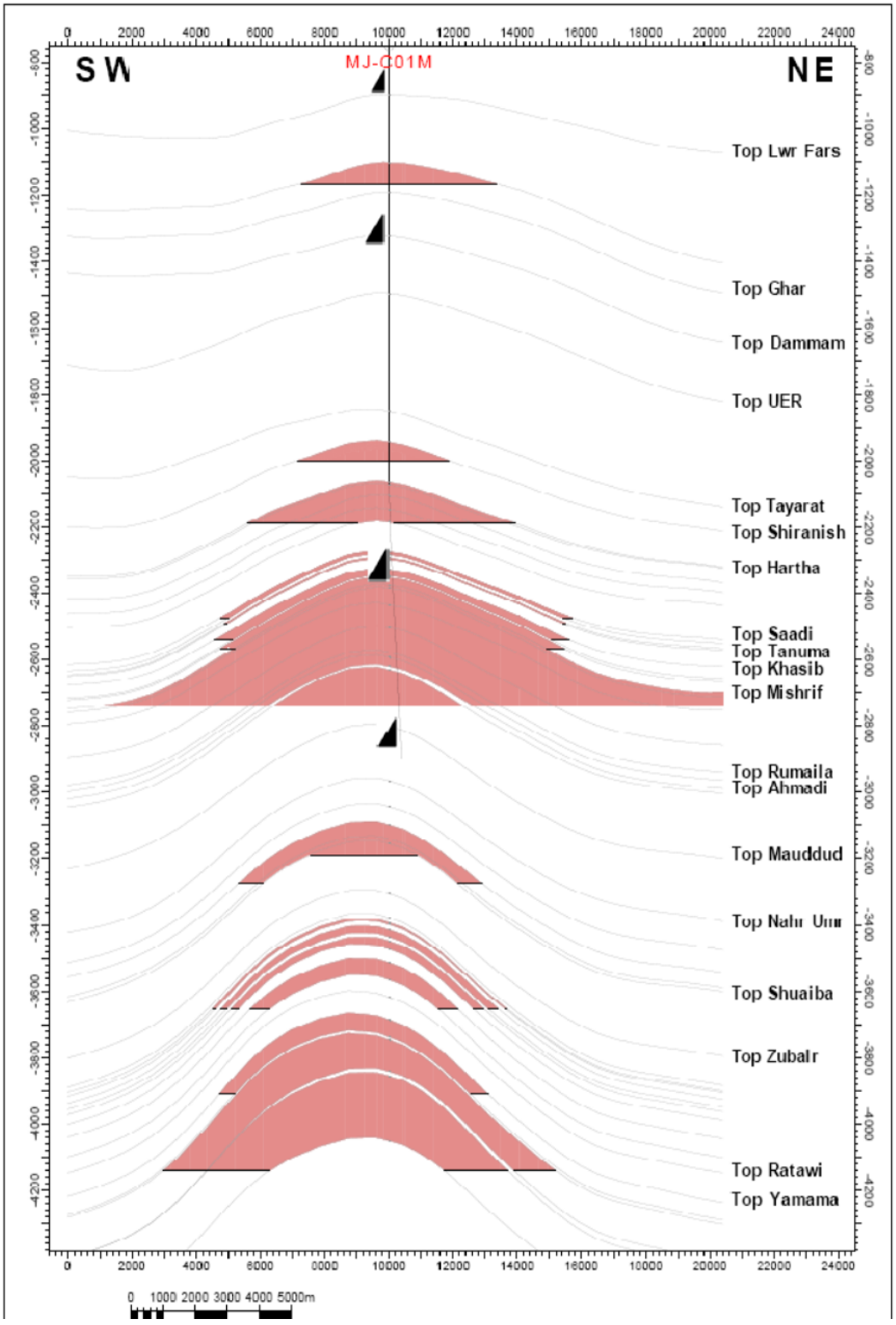

Figure 1.3: The geological prognosis of the E oilfield

1.3 DATA UTILIZATION FOR WELLBORE-STABILITY ANALYSIS

The utilization of available data for wellbore-stability analysis is discussed in the following subsections.

1.3.1 Well Logging Data. Well logging data is available for several wells drilled in the study field. Well log data were used to build petrophysical models. In addition, Image and Sonic log data collected in a limited number of wells were utilized to obtain in- situ stress magnitudes as well as stress orientations and to estimate the level of stress anisotropy. Moreover, the image logs were used to correlate the drilling data and observed borehole conditions to identify the specific intervals causing wellbore-stability issues.

1.3.2 Daily Drilling Reports. Daily drilling reports can be a helpful source to identify unstable intervals nad causes for rock failure when the well-log data is not available. Observed challenges during the drilling process such as string over-pulls, dragging, and mud losses were correlated with caliper and well image log data to identify the unstable intervals. The time effect associated with the chemical interactions was indirectly implied from the drilling performance and the caliper data.

1.3.3 Daily Mud Reports. Daily mud reports were utilized to identify the mud characteristics: MW, rheological properties, and sand percent. In addition, the report describe the formation's cuttings size and provides an indirect clue to the hole cleaning issues during drilling of the directional wells.

1.3.4 Daily Mud Logging Reports. Daily mud logging reports were used to acquire input data for petrophysical modeling. Also, mud logging reports were used to identify the high pore pressure zones. The size and shape of cuttings were used to verify the active wellbore- failure mechanism taking place in the field to make a critical decision about whether to increase mud weight or to hold it at the same level. Moreover, gas show readings were used to pinpoint the pore pressure for the hydrocarbon-saturated shale intervals.

1.3.5 Primary Cementing Reports. An indirect utilization of cementing reports is one of the correlating factors for predicting a maximum allowable Equivalent Circulation Density (ECD) to drill a particular section.

1.3.6 End-of Well Report and Non-Productive Time Analyses. End-of-report and non-productive time analyses were used to estimate an economical optimization of the drilling projects for the field development in the oil-field.

PAPER

I. WELLBORE STABILITY EVALUATION FOR THE MISHRIF FORMATION

ABSTRACT

During drilling operations for the E oilfield in the Mishrif formation in southern Iraq stuck pipe (as a geomechanical problem) and differential sticking (related to pressure management) have been identified as significant problems for several wells. In this study, a 1-D mechanical earth model (MEM) of the Mishrif formation is compiled based on the in situ state of stress and rock strength parameters, and is utilized to assess the contribution of borehole collapse leading to the stuck pipe problems. The results of this study show that the operating minimum mud weight has been chosen without considering geomechanical principles. The results of this study document the prediction of the minimum mud weight based on three different failure criteria. The results obtained from the Mogi–Coulomb failure criterion indicate that all wells experiencing collapse and associated stuck pipe were drilled along azimuths which promote wellbore collapse and have been drilled with too low of a mud weight. The 1D MEM approach presents minimum mud weight design and optimal drilling trajectories to mitigate wellbore collapse for future wells. Based on the horizontal stress orientations, this study recommends well azimuths along the minimum horizontal stress direction with inclinations higher than 40°. In addition, the 1D MEM approach can also be used to mitigate the occurrence of differential sticking as observed for several wells in the Mishrif Formation. The results presented show that all wells experiencing differential sticking have been drilled with a mud weight higher than suggest-

-ed by the Mogi-Coulomb criterion. The presented study shows that 1D MEMs are an important tool to both assess and address existing wellbore stability problems and to provide guidance for future well plans for better drilling efficiency by reducing non-productive time.

1. INTRODUCTION

It is estimated that more than 60% of the world's oil and 40% of the world's gas reserves are held in carbonate reservoirs. The Arabian plate, as an example, is dominated by carbonate fields, with around 70% of oil and 90% of gas reserves held within these reservoirs (Schlumberger, 2016). The Mishrif Formation in southern Iraq represents heterogeneous organic detrital limestones, with beds of algal, rudist, and coral reef limestones, capped by limonitic fresh water limestones (Aqrawi et al., 2005, Jassim and Goff, 2006). The thickness of the formation is around 237 m, ranging from the top 2393 m true vertical depth (TVD) to the bottom of the formation at 2630 m TVD.

For improved drilling and production efficiency, non-vertical, deviated production wells are adopted in a particular oilfield in the Mishrif Formation (termed Oilfield E in this paper). In some cases, deviated boreholes are drilled to reach a substantial distance horizontally away from the drilling location (Schroeter et al, 1989). Moreover, the deviated boreholes are essential to reach locations that are not accessible through vertical boreholes due to Explosive Remnants of War (ERW; Huysduynen et al., 2014). However, drilling non-vertical boreholes accounts for a variety of problems, such as cuttings transport, casing setting and cementing, and drill string friction. In the E oilfield, many wells were characterized by differential sticking (Helmick and Longley, 1957) across the Mishrif formation and also had some challenges during in-hole cleaning as the “J” and “S” shaped wells had a tangent section between 20^{o} and 42^{o} degree inclination. Moreover, several wells experienced significant wellbore stability problems with stuck pipe as a consequence of borehole collapse being the most frequent (Charlez, 1991). The wellbore stability problems were observed in wells with azimuths ranging from 9° to 310°. A review of the drilling

operation data shows that the used mud weight window was based on formation pore pressure and formation breakdown pressure only. Detailed geomechanical calculations necessary to determine the safe mud pressure window for deviated wellbore trajectories (e.g. Peska and Zoback, 1995), including the in-situ stress magnitudes, rock strength properties and oriented wellbore data, were not considered.

This study utilizes a 1D MEM approach (e.g. Kristiansen, 2007; Gholami et al., 2014) in order to determine the collapse pressure (i.e. minimum mud weight) for the Mishrif Formation. The geomechanical model includes the in-situ principal stresses and their orientations obtained from wireline logging measurements, measurements while drilling (MWD), and leak off tests (LOT). Rock strength properties are obtained from empirical equations and extended leak off tests. Three different failure criteria, the Mohr-Coulomb, Mogi-Coulomb, and Modified Lade criteria, representing a conservative, realistic and optimistic criterion (Mohr, 1900; Ewy, 1999; Al-Ajmi and Zimmerman, 2005; Maleki, et al., 2014; Rahimi and Nygaard, 2015) are investigated in order to analyze the existing wellbore stability and differential sticking problems for 8 wells (termed Wells A – H), and to determine feasible (i.e. safe) drilling trajectories (i.e. azimuths and inclinations) and mud weight conditions for many different wells in the Mishrif Formation.

2. METHODOLOGY

An analysis of the optimal mud weight for drilling a new well through depleted reservoirs requires a field-specific geomechanical model, termed a 1D Mechanical Earth Model (MEM), that consists of characterization of the elastic parameters, rock strength properties, pore pressure and in-situ stresses. The components of the 1D MEM for the Mishrif Formation are derived from daily drilling reports, daily mud reports, formation integrity tests (FIT), and wireline well logs.

2.1 IN-SITU STRESSES

Stable drilling trajectories are directly dependent on the knowledge of the in-situ state of stress (Bell, 1996). Since detailed information about the in-situ stress regime of the Mishrif formation is unknown (or confidential), the assumed Andersonian state of stress (Jaeger et al, 2007) is determined by a procedure, which initially determines the vertical stress from wireline density logs, followed by minimum horizontal stress determination from extended leak-off tests and the estimation of the maximum horizontal stress using borehole breakout data (Zajac and Stock, 1992), which in turn is validated by stress polygon analysis (Zoback, et al. 1986; Moos and Zoback 1990). Stress orientations are derived from breakout orientations (e.g. Zoback et al., 1985; Bell and Babcock, 1986; Mastin, 1988; Tingay et al., 2011).

2.1.1 Vertical Stress. The weight of the overburden is calculated by integrating the bulk density log (shown in Appendix A) based on Eq. 1.

$$\sigma v = \int_0^z \rho g \, dz \tag{1}$$

where z is vertical depth, g is the gravitational acceleration constant, and ρ is the rock bulk density at a specific depth. The vertical stress in the Mishrif Formation ranges from 59 MPa to 66 MPa (based on data from 8 wells in the Mishrif Formation; Table 2.1).

Table 2.1: MEM parameters for eight wells in Mishrif formation

MEM parameters	Well A	Well B	Well C	Well D	Well E	Well F	Well G	Well H
σ_v (MPa)	59.6	60.3	56.7	61.5	62.7	62.6	61.2	63.5
σ_h (MPa)	32.0							
σ_H (MPa)	53.6	45.0	43.4	56.6	57.9	52.1	65.5	50.5
σ_H orientation (degree)	51.0							
P_o (MPa)	26.0	26.0	26.0	26.0	26.0	26.0	26.0	26.0
UCS (MPa)	47.8	37.3	29.1	60.9	60.9	47.6	99.5	47.6
T_o (MPa)	8.00							
φ (degree)	21.02		21.61				25.53	

2.1.2 Minimum Horizontal Stress. The minimum horizontal stress is determined by an extended leak-off test (Zoback et al., 1985) conducted in Well A of the E Oilfield. The magnitude of the minimum horizontal stress (σ_h) is represented either by the instantaneous shut-in pressure (ISIP; if low viscosity fluids such as water or thin oils are used) or the fracture closure pressure (FCP; if higher viscosity fluids such as oil are used) on the mini-frac test plot (Figure 2.1.; Zoback 2010). As the fracturing fluid for the mini-frac test in the Mishrif formation was water, the ISIP is used to determine the minimum horizontal stress of 32 MPa at a depth of 2534 m (Figure 2.1; Table 2.1).

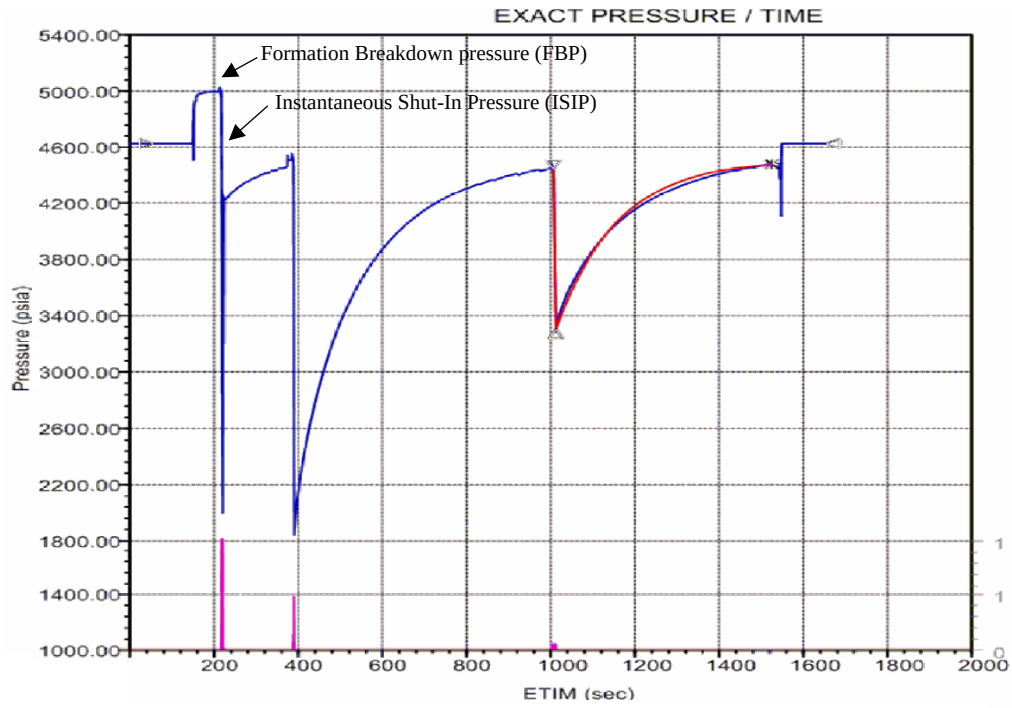

Figure 2.1: Extended leak-off test in Well A to determine the minimum horizontal stress, S_h for the Mishrif formation. The ISIP indicates a S_h of 32 MPa

2.1.3 Pore Pressure. The Mishrif Formation is characterized by highly variable pore pressures. Figure 2.2 shows pore pressure measurements from more than 40 wells. The pore pressure measurements are based on repeat formation tests (Stewart and Wittmann, 1979) for the Oilfield E including the Mishrif Formation and over- and underlying formations (Figure 2.2). Due to inconsistencies in the measured pore pressure values (i.e. the pore pressure data distribution represents more than 40 wells) resulting in maximum (Max P_p) and minimum pore pressure (Min P_p) distributions, drilling operations were based on an interpolated pore pressure across the whole field (Int P_p). This interpolated pore pressure is also used in the following calculations for the updated mud weight window.

Figure 2.2. also shows the formation breakdown pressure (FBP) obtained from leak-off tests for more than 40 wells. Similar to the pore pressure measurements an interpolated FBP is calculated based on the maximum FBP (Max FBP) and minimum FBP (Min FBP) measurements. The interpolated pore pressure and FBPs were subsequently used to calculate the operating mud weight window.

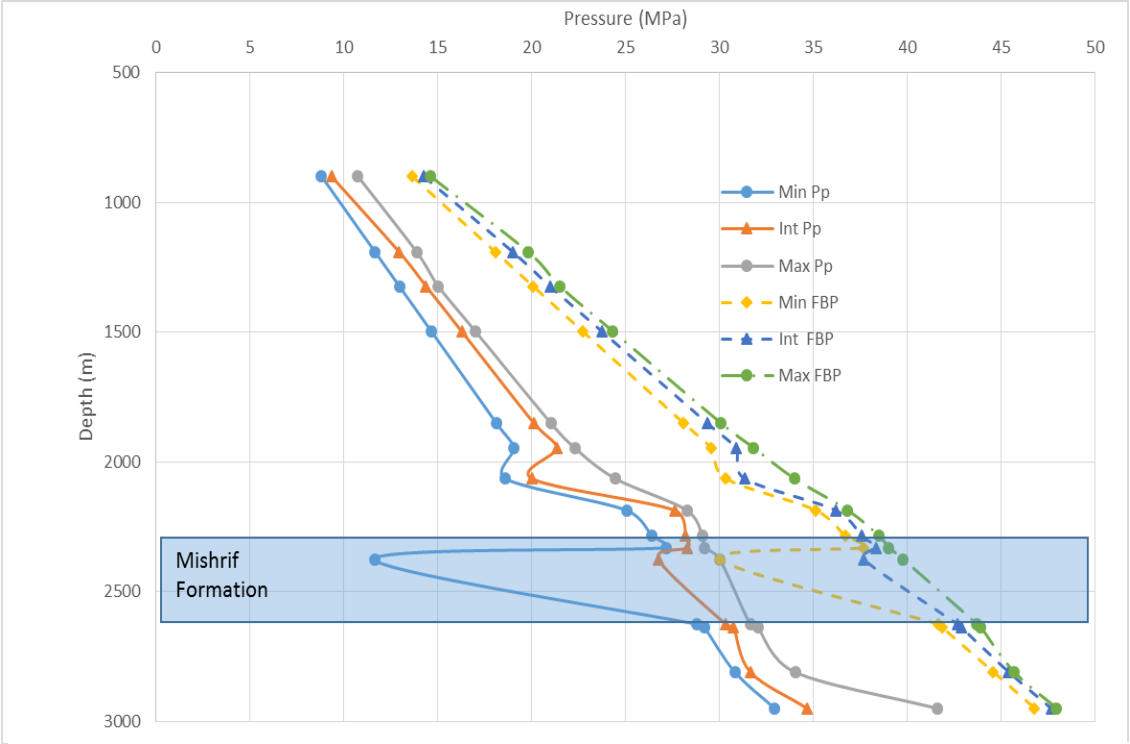

Figure 2.2: The E Field mud pressure window is based on interpolated pore pressure and formation breakdown pressures. Pore pressures in the Mishrif Formation range from 16 MPa to 29 MPa

2.1.4 Maximum Horizontal Stress. As the maximum horizontal stress magnitude cannot be measured directly, several methods to obtain an estimate are employed. The first estimate is obtained by data obtained from the extended leak-off test (Haimson and Fairhurst, 1969). For a hydraulic fracture to propagate, the formation breakdown pressure is given by:

$$FBP = 3\sigma_h - \sigma_H + T_0 - P_p \quad (2)$$

the tensile strength, T_0, can be estimated from repeat cycles of an extended leak-off test (Fjaer, 1992; T_0=8 MPa for the Mishrif Formation), σ_H is given by:

$$\sigma_H = 3\sigma_h - FBP + T - P_p \quad (3)$$

For the extended leak-off test conducted in well A in the Mishrif Formation σ_H = 41 MPa. Since measurements/estimates for pore pressure, FBP and tensile strength are also available (based on extended leak-off tests) for wells B-H, assuming that σ_h from Well A applies for the whole field, additional stress magnitude estimates for σ_H (for wells B-H) can be obtained (Table 2.1).

The second estimate for σ_H is obtained using the technique of circumferential wellbore modeling (Zoback et al., 2003). The fact that drilling induced tensile failure is not observed in any well in the Mishrif Formation requires:

$$3\sigma_h - \sigma_H - P_p - P_i > -T_0 \quad (4)$$

With the previously determine magnitudes for σ_h, pore pressure, mud pressure and tensile strength, σ_H > 46MPa in the Mishrif Formation.

A similar constraint on σ_H can be obtained considering the observation of breakouts in a deviated well following Zoback and Peska (1995). However, since the following analysis evaluates the influence of three different failure criteria (Modifier Lade, Mohr-Coulomb, Mogi-Coulomb) on the observed well stability problems in the E oilfield, Zoback and Peska's (1995) procedure would have to be conducted for the three different failure criteria. Moreover, Fjaer et al. (2008) have shown that six different permutations of

the axial, hoop and radial stress have to be considered in order to map the occurrence of instability regions in a deviated wellbore. Such an extensive analysis of the estimation of σ_H is beyond the scope of this study and will be considered in a separate contribution. For the assumption of a vertical well (for a Mohr-Coulomb failure criterion) a simple estimate of σ_H can be obtained by requiring:

$$\sigma_1 \geq UCS + \sigma_3 \frac{1 + \sin\varphi}{1 - \sin\varphi} \tag{5}$$

Where $\sigma_1=\sigma_{\Theta\Theta}$ (hoop stress), $\sigma_3=\sigma_{rr}$ (radial stress), UCS is the unconfined compressive strength, and Φ is the coefficient of internal friction. This gives:

$$3\sigma_H - \sigma_h - P_p - P_i \geq UCS + \left(P_i - P_p\right)\frac{1 + \sin\varphi}{1 - \sin\varphi} \tag{6}$$

where P_i represents the wellbore fluid pressure. Hence, σ_H can be estimated by:

$$\sigma_H \geq \frac{1}{3}\left[UCS + \left(P_i - P_p\right)\frac{1 + \sin\varphi}{1 - \sin\varphi} + \sigma_h + P_p + P_i\right] \tag{7}$$

The data for the Mishrif formation for well A yields $\sigma_H \geq 53\ MPa$, which coincides with the previous estimate of σ_H > 46MPa. Since breakouts and wellbore collapse is observed in several wells in the Mishrif formation, $\sigma_H = 53\ MPa$ is used for the subsequent wellbore stability analysis.

In addition, to further evaluate the previous constraints for σ_H, stress polygon analysis (Figure 2.3; Zoback et al., 1986) shows that the σH magnitudes determined favor an extensional (i.e. normal faulting) stress regime and that the σ_H magnitudes are on the periphery of the polygon, which is often observed for crustal stresses in frictional equilibrium (Zoback, 2010).

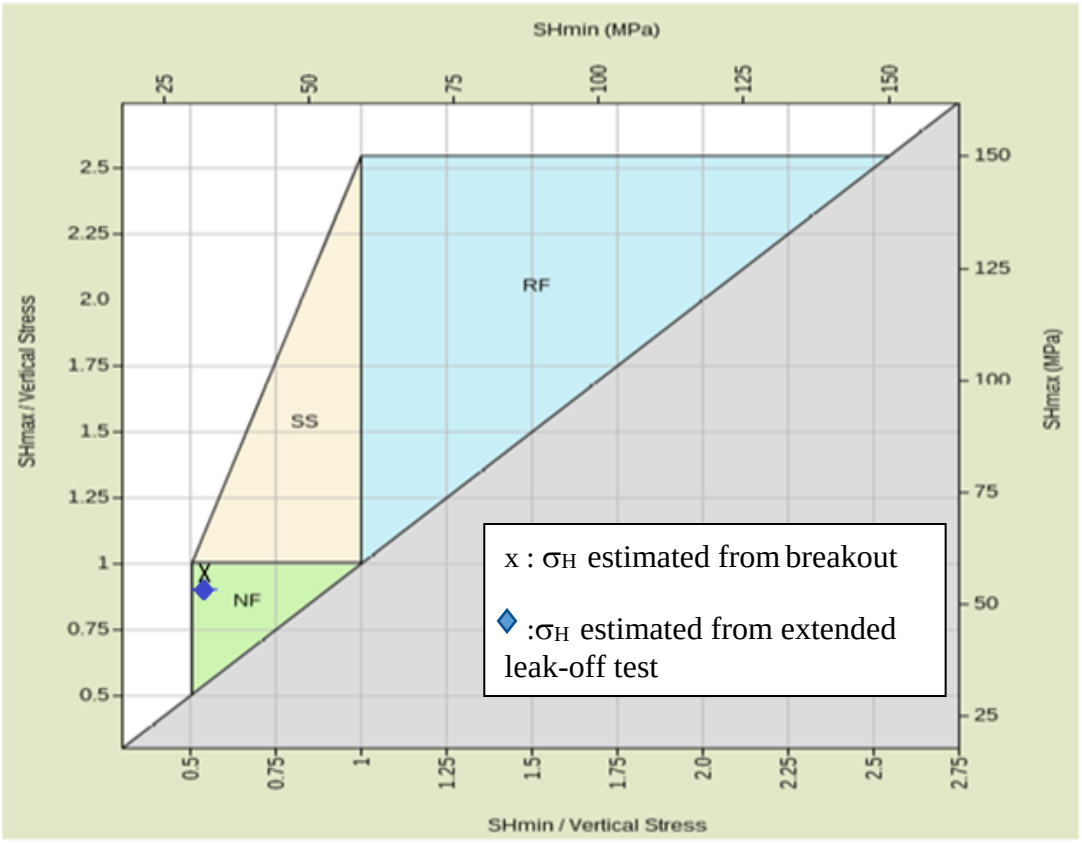

Figure 2.3: Mishrif Formation stress polygon analysis showing that the inferred stress magnitudes document a normal faulting stress regime

2.1.6 The Orientation of Maximum Horizontal Stresses. Stress orientations of σ_H were determined from borehole breakouts interpreted from resistivity image logs and four-arm caliper data. By definition, the maximum horizontal stress direction is perpendicular to the breakout azimuth (Zoback et al., 1985). Breakout orientation data in the Mishrif Formation determined from Formation Micro-Imager (FMI) log data (Figure 2.4.) comprises 6 breakout zones of a combined length of ~7m yielding a maximum horizontal stress direction of 51°±12° (Figure 2.5.a). Following the quality criteria defined by the world-stress-map data base (Appendix B, Zoback, 2010), Quality B is assigned. Based on interpretation of the 4-arm caliper log data (Jarosiński, 1998), only one breakout

of 0.5m length could be identified, yielding a maximum horizontal stress direction of 54° (i.e. resulting in Quality D; Figure 2.5.b). While the stress orientation data is not extensive, a close correlation to nearby stress measurements from an oilfield in Kuwait (Azim et al., 2011), which shows a maximum horizontal stress direction of 45°, was obtained.

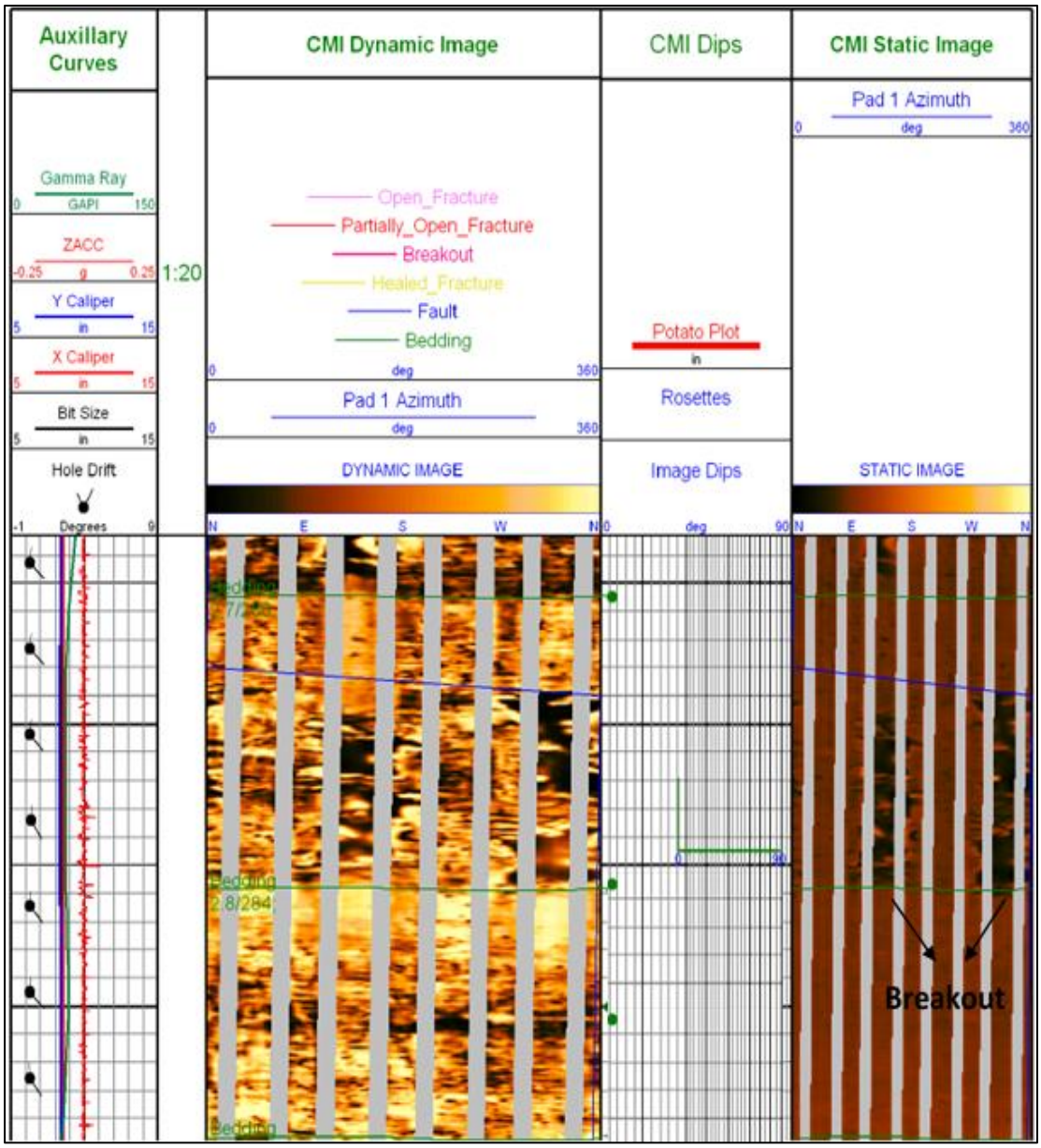

Figure 2.4: FMI log (well A) showing an exemplary borehole breakout oriented towards 146ºN and 328 ºN.Indicating an approximately NE-SW maximum horizontal stress orientation

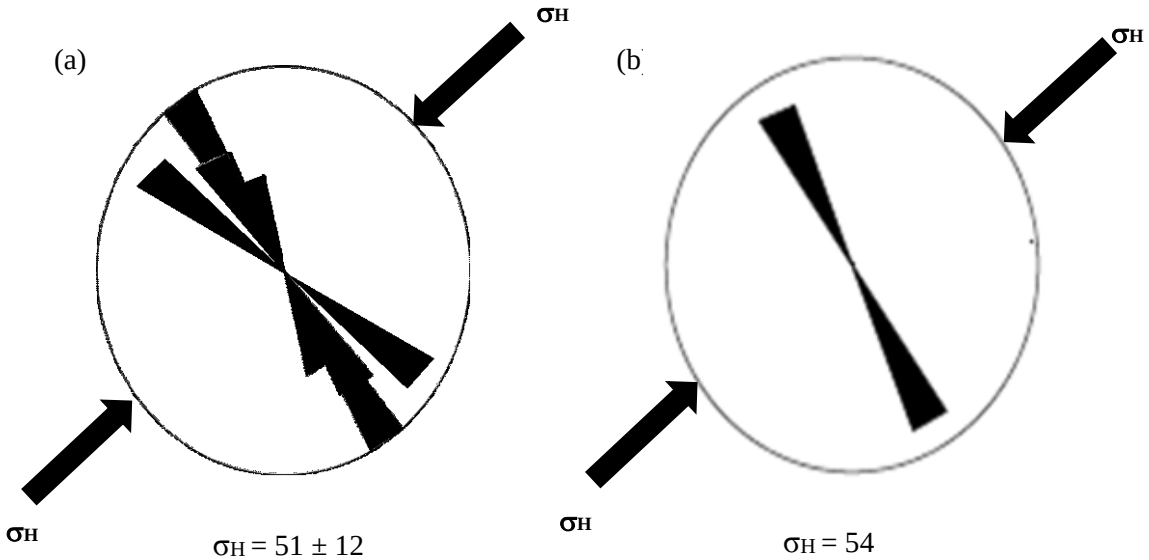

Figure 2.5: Breakout orientations for Mishrif formation; (a) Shows the breakout orientations obtained from the FMI log, (b) Shows the Breakout orientations obtained from the four arm caliper log

2.2 ELASTIC PARAMETERS

Due to the absence of laboratory core measurements and S-wave velocities not being recorded on the sonic log, the Poisson's ratio is assumed to be 0.25.

2.3 ROCK STRENGTH

Since the following wellbore stability analyses are based on the Mohr-Coulomb, the Modified Lade and the Mogi-Coulomb failure criteria, the rock strength parameteres of cohesion (determined from the unconfined compressive strength), S_o, internal friction angle, ϕ, and tensile strength, T_0, need to be determined.

2.3.1 Unconfined Compressive Strength (UCS). Due to the absence of laboratory core measurements, UCS is determined using empirical relationships based on

wireline logging measurements (Chang et al., 2006). For limestone, UCS is related to the porosity by (Chang et al., 2006):

$$UCS = 143.8 \exp(-6.95\emptyset) \quad (8)$$

The porosity is determined directly from the Neutron log. For the Mishrif Formation data from eight wells gives UCS in the range of 29 to 99.5 MPa (Table 1). The UCS can be related to the cohesion and the angle of internal friction by Eq. 9 (Al-Ajmi and Zimmerman, 2005).

$$UCS = (2 \text{ So } cos\phi)/(1 - \sin\phi) \quad (9)$$

Where S_o is the rock cohesion and ϕ is the internal friction angle.

2.3.2 Internal Friction Angle. It can be determined by correlating physical laboratory test data to a typical downhole log (commonly acoustic or density) by an empirical equation. Due to the lack of core data the internal friction angle can be estimated from Eq. 10-11 (Plumb 1994).

$$\Phi = 26.5 - 37.4(1 - NPHI - V_{shale}) + 62.1\,(1 - NPHI - V_{shale})^2 \quad (10)$$

where NPHI is the neutron porosity, and V_{shale} is the volume of shale obtained by

$$V_{shale} = \frac{GR - GR_{min}}{GR_{max} - GR_{min}} \quad (11)$$

For the Mishrif Formation ϕ is in the range of 21° to 25° (Table 2.1).

2.3.3 Tensile Strength. Due to the absence of a Brazilian strength test, T_o is estimated from the extended leak-off test (Torres et al., 2003), for which T_o can be estimated by the difference between the FBP and ISIP as shown in Fig. 1. For the Mishrif Formation a tensile strength of 8 MPa is determined (based on data from Well A; (Table 2.1).

3. CONSTITUTIVE MODELS AND STRESSES AROUND A DEVIATED WELL

Before drilling a well, a stress state exists in the rock formation in terms of the principal stresses σ_v, σ_H, and σ_h. After the hole is drilled, it's filled with a drilling mud exerting a pressure (p_w). Since the wellbore may take any orientation, therefore these stresses are to be transformed to a new Cartesian coordinate system σ_x, σ_y, and σ_{zz} taking in account the wellbore inclination from vertical (i) and the geomechanical azimuth (α) as shown in Eq. 12 (Aadnoy, 1989; Aadnoy and Looyeh, 2011).

$$\begin{bmatrix} \sigma x \\ \sigma y \\ \sigma zz \\ \tau\, xy \\ \tau\, xz \\ \tau\, yz \end{bmatrix} = \begin{bmatrix} cos^2\varphi cos^2\gamma & sin^2\varphi cos^2\gamma & sin^2\gamma \\ sin^2\varphi & cos^2\varphi & 0 \\ cos^2\varphi sin^2\gamma & sin^2\varphi sin^2\gamma & cos^2\gamma \\ -0.5sin2\varphi cos\gamma & 0.5sin2\varphi cos\gamma & 0 \\ 0.5cos^2\varphi sin2\gamma & 0.5sin^2\varphi sin2\gamma & -0.5sin2\gamma \\ -0.5sin2\varphi sin\gamma & 0.5sin2\varphi sin\gamma & 0 \end{bmatrix} \begin{bmatrix} \sigma H \\ \sigma h \\ \sigma v \end{bmatrix} \quad (12)$$

Figure 3.1 shows that the principal stresses around the wellbore are represented in terms of σ_r, σ_Θ, and σ_z the σ_x, σ_y, and σ_{zz} stresses and the shear components for circular shape of wellbore. Where the borehole deviation effect is taking in account as in Eq. 13 through Eq. 18 (Fjaer, 1992).

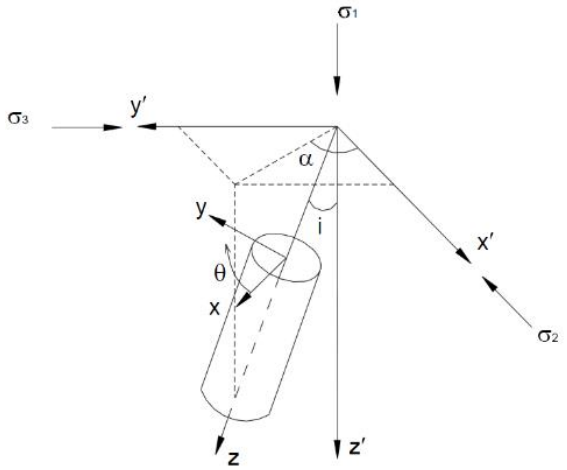

Figure 3.1: Stress transformation system for a deviated borehole

$$\sigma_r = \frac{1}{2}(\sigma_x + \sigma_y)\left(1 - \frac{a^2}{r^2}\right) + \frac{1}{2}(\sigma_x - \sigma_y)\left(1 + 3\frac{a^4}{r^4} - 4\frac{a^2}{r^2}\right)cos2\theta + \tau_{xy}\left(1 + 3\frac{a^4}{r^4} - 4\frac{a^2}{r^2}\right)sin2\theta + \frac{a^2}{r^2}P_w \quad (13)$$

$$\sigma_\theta = \frac{1}{2}(\sigma_x + \sigma_y)\left(1 + \frac{a^2}{r^2}\right) - \frac{1}{2}(\sigma_x - \sigma_y)\left(1 + 3\frac{a^4}{r^4}\right)cos2\theta - \tau_{xy}\left(1 + 3\frac{a^4}{r^4}\right)sin2\theta - P_w\frac{a^2}{r^2} \quad (14)$$

$$\sigma_z = \sigma_{zz} - 2v(\sigma_x - \sigma_y)\frac{a^2}{r^2}cos2\theta - 4v\,\tau_{xy}\,\frac{a^2}{r^2}sin2\theta \quad (15)$$

$$\tau_{r\theta} = \left[\frac{1}{2}(\sigma_x - \sigma_y)sin2\theta + \tau_{xy}\,cos2\theta\right](1 - 3\frac{a^4}{r^4} + 2\frac{a^2}{r^2}) \quad (16)$$

$$\tau_{\theta z} = (-\tau_{xz}sin\theta + \tau_{yz}\,cos\theta\,)(1 + \frac{a^2}{r^2}) \quad (17)$$

$$\tau_{rz} = (\tau_{xy}\,cos\theta + \tau_{yz}\,sin\theta\,)(1 - \frac{a^2}{r^2}) \quad (18)$$

where σ_Θ is the tangential (hoop) stress, σ_r is the radial stress and σ_z is the axial stress induced around the wellbore at a distance (r) away from a wellbore with a radius of (R). The angle Θ is measured clockwise from σ_H direction and varies from 0° to 360°. The Kirsch equations corresponding to the borehole wall (where r = R) are simplified to Eq. 19 through Eq.21.

$$\sigma_r = P_w \tag{19}$$

$$\sigma_\theta = (\sigma_H + \sigma_h) - 2(\sigma_H - \sigma_h)cos2\theta - P_w \tag{20}$$

$$\sigma_z = \sigma_V - 2\upsilon(\sigma_H - \sigma_h)cos2\theta \tag{21}$$

According to the previous equations, σ_r and σ_Θ are functions of angle θ. This angle indicates the orientation of the stresses around the wellbore circumference, and varies from 0° to 360°. Inspection of these two equations reveals that both tangential and axial stresses reach a maximum value at $\Theta=\pm\pi/2$ and a minimum value at $\Theta=0, \pi$. The above equations also show that the tangential and radial stresses are functions of mud pressure, p_w. Therefore, any change in the mud pressure will only affect the σ_r and σ_Θ. As it is well-known, two main stability problems are usually occurred during drilling: shear and tensile failures. Since we are concerned with the changes in σ_r and σ_Θ with respect to pw, there will be two possible scenarios: either $\sigma_\Theta > \sigma_r$, or $\sigma_r > \sigma_\Theta$. When pw increases (or equivalently, σ_r), it reduces the magnitude of σ_Θ to a limit where it becomes zero, i.e. the beginning of inducing fracture into the formation at the point where $\Theta=0, \pi$. Therefore, the upper limit of the mud pressure, pw (fracture), is associated with fracturing. In general, depending on the order of the magnitude of the induced stresses around the wellbore, there will be three alternative scenarios that should be considered to determine the maximum allowable mud pressure.

While, the principal effective stresses around the wellbore are given by Eq. 22 and Eq.23 (Zoback, 2010).

$$\sigma_{tmax} = \frac{1}{2}\left(\sigma_z + \sigma_\theta + \sqrt{(\sigma_z - \sigma_\theta)^2 + 4\tau_{\theta z}^2}\right) \tag{22}$$

$$\sigma_{tmin} = \frac{1}{2}\left(\sigma_z + \sigma_\theta - \sqrt{(\sigma\sigma_z - \sigma_\theta)^2 + 4\tau_{\theta z}^2}\right) \tag{23}$$

4. ROCK FAILURE CRITERIA FOR WELLBORE STABILITY ANALYSIS

Rock failure criterion specifies stress conditions at failure, where many empirical approaches have been developed to predict rock and formation failure. These tests have been classified based on many characteristics. But the most important classification is involves considering the effect of intermediate principal stress on the rock strength. For example the Mohr-Coulomb criterion was classified as very conservative criteria in wellbore stability evaluation it's not examine the effects of intermediate principal stress. In contrast, Mogi-Coulomb and Modified Lade describe the influence of the intermediate principal stress on rock strength with different mean misfit to various rocks (Colmenares and Zoback, 2002), and therefore on wellbore stability to provide a solution for critical mud weight, for any wellbore orientation (Maleki, et al., 2014).

4.1 MOHR-COULOMB FAILURE CRITERION

The Mohr-Coulomb failure criterion is the most commonly used failure criterion in mechanical earth modeling, which does not consider the effect of the intermediate principal stress in contrast to the triaxial stress state of rock. The Mohr-Coulomb criterion is based on the assumption that $f(\sigma)$ is a linear function of σ as shown in Eq. 24 and Eq.25 (Mohr, 1900):

$$\tau = \mu\sigma + S_o \tag{24}$$

$$\mu = tan\phi \tag{25}$$

Regarding the principal stresses, the Mohr-Coulomb failure criterion can be expressed in Eq. 26.

$$\sigma_1 = q\sigma_3 + UCS \tag{26}$$

Where:

$$q = \frac{1 + sin\phi}{1 - sin\phi} \tag{27}$$

$$UCS = \frac{2S\ cos\phi}{1 - sin\phi} \tag{28}$$

4.2 MOGI-COULOMB FAILURE CRITERION

It was first introduced by Al-Ajmi and Zimmerman (Al-Ajmi and Zimmerman, 2005 ; 2006). This failure criterion considers the effect of the intermediate principal stress. The Mogi-Coulomb criterion can be formulated in Eq. 29.

$$\tau_{oct} = \kappa + m\sigma_{oct} \tag{29}$$

Where τ_{oct} and σ_{oct} are the octahedral shear and normal stresses, defined as in Eq.30 through Eq.32.

$$\tau_{oct} = \frac{1}{3}\sqrt{(\sigma_1 - \sigma_2)^2 + (\sigma_1 - \sigma_3)^2 + (\sigma_2 - \sigma_3)^2} \tag{30}$$

$$\sigma_{oct} = \frac{1}{3}(\sigma_1 + \sigma_2 + \sigma_3) \tag{31}$$

$$\tau_{oct} = a + b\sigma_{m,2} \tag{32}$$

where:

$$\sigma_{m,2} = \frac{\sigma_1 + \sigma_3}{2} \tag{33}$$

$$a = \frac{2\sqrt{2}}{3} \mathrm{So} \cos \emptyset \tag{34}$$

$$b = \frac{2\sqrt{2}}{3} sin\ \emptyset \tag{35}$$

4.3 MODIFIED LADE FAILURE CRITERION

The Modified Lade failure criterion is a three-dimensional failure criterion that was originally proposed for cohesion-less sands. Then the criterion was adopted for analyzing rocks with finite values of cohesion ($S_{o)}$ and T_o by Lade (1984) and such a formulation was later linked (Ewy, 1999) with the standard rock mechanics parameters such as ϕ and S_o as shown in Eq.s 36 through 38.

$$\frac{(I_1')^3}{I_3'} = 27 + \eta \tag{36}$$

Where, I_1' and I_3' are stress invariants.

$$I_1' = (\sigma_1 + S - P_o) + (\sigma_2 + S - P_o) + (\sigma_3 + S - p_o) \tag{37}$$

$$I_3' = (\sigma_1 + S - P_o)(\sigma_2 + S - P_o)(\sigma_3 + S - p_o) \tag{38}$$

Where, S is related to the cohesion of the rock, and η represents the internal friction. Parameters S and η can be derived directly from the Mohr-Coulomb cohesion S_o and internal friction angle ϕ by Eq. 39 and Eq.40.

$$S = \frac{S_o}{tan\phi} \tag{39}$$

$$\eta = \frac{4tan^2\phi(9 - 7\sin\phi)}{1 - sin\phi} \tag{40}$$

Note that S_o can be linked to C_o and ϕ through $S_o = C_o/2q^{1/2}$, whereas $q=\tan^2(\pi/4+ \phi/2)$.

3. WELLBORE STABILITY

3.1 DRILLING CHALLENGES

Due to the heterogeneity of the Mishrif reservoir, the formation pore pressure fluctuates across the entire reservoir zone, which causes localized fluctuations in the near-wellbore stresses. Under this scenario, high-enough mud-weight values (while maintaining overbalanced drilling conditions) are required to minimize breakout severity (i.e. shear failure: e.g. Zoback, 2010 and references therein). However, in the case of low reservoir pore pressure (as also observed in the Mishrif Formation), the pore pressure might be close to hydrostatic or sub-hydrostatic; thus, a higher mud weight is likely to cause a large overbalance, increasing the chances of getting differentially stuck while drilling across these reservoirs (Helmic, 1957). It must be restated that the interpolated pore pressure was used to calculate the operating mud weight window.

Due to the uncertainty in the distribution of the pore pressure along the planned trajectory, the predicted mud weight will have uncertainties both for minimizing breakouts (lower limit) and managing differential sticking (upper limit). Because a drilling problem could result from one or a combination of these parameters, an integrated approach to select the optimum mud weight between the minmimum mud weight required to prevent collapse failure (i.e. stuck pipe) and the maximum overbalance allowed to prevent the differential sticking occurance, is used here.

3.2 COLLAPSE PRESSURE

The minimum mud weight, i.e. also termed collapse pressure, is determined based on the compiled 1D MEM for all possible wellbore trajectories (Peska and Zoback, 1996).

The equations for the calculation of the required tangential wellbore stresses in an arbitrarily oriented wellbore are given in detail in Peska and Zoback (1996) and Zoback (2010) and are therefore not repeated here. Based on the MEM, three different failure criteria (Mohr-Coulomb, Mogi-Coulomb, and Modified Lade) are used to evaluate the risk of borehole collapse. Figure 6 and 7 show the collapse pressure for two of the eight wells in Field E for different wellbore orientations.

3.3 DIFFERENTIAL STICKING

Differential sticking can result when pressure from an overbalanced mud column acts on the surface area of the drill string against a filter cake deposited across a permeable formation. The surface area of the pipe that is embedded into the mud cake has a pressure equal to the pore pressure acting from one direction while the hydrostatic pressure acts in the other direction. When the hydrostatic pressure in the wellbore is higher than the formation pressure, the pressure differential forces the pipe towards the borehole wall. This usually occurs along the drill collars because there is less annular clearance to begin with, the drill collars usually have larger diameter, which increases the crossectional area that is in contact with the borehole, and the drill collars are the first section of the pipe to encounter the permeable formation (Rehm and et al., 2008). The best method to limit the risk of differential sticking is by using the minimum mud weight (Helmic and Longgley, 1957).

4. RESULTS AND DISCUSSION

An analytical model incorporating three failure criteria is adopted to help predicting the mud weight window as a function of the wellbore inclination and azimuth. This model is applied to analyze the mechanical stability of eight deviated wells in the Mishrif formation oilfield E (wells A-H). Two wells (A and B) are considered as exemplary studies in order to address the geomechanical problems of stuck pipe (Well A) and differential sticking (Well B), respectively (Table 4.1). Since comparing different failure criteria is not the objective of this study, the Mohr-Coulomb, the Mogi-Coulomb and the Modified Lade criterion are used as examples of including/excluding the intermediate principal stress on wellbore stability (Rahimi and Nygaard, 2015).

Figures 4.1. and 4.2. show stereographic contours (for all possible azimuths and inclinations) for the minimum mud weight for Well A and B, respectively using the three different failure criteria (Peska and Zoback, 1995). Both figures indicate the most stable drilling azimuth (i.e. requiring the lowest mud weight) is parallel to the minimum horizontal stress for inclinations of more than 50°. For the case of drilling in the direction of the maximum horizontal stress a higher mud weight is required to keep the well stable. For inclinations up to 30^{o}, the well azimuth only has a slight effect on the mud weight.

For Well A (drilled with a mud weight of 1.1 specific gravity (sg)), the results show (independent of failure criteria) that the field operator used a mud weight less than required for the planned azimuth and inclination (triangle symbol in Figure 4.1.a, b, c) which led to wellbore collapse. As the results for the various failure criteria show (for the actual drilled well), the Modified Lade criterion (Figure 4.1.a) predicts a mud weight of

1.175 sg. The Mohr-Coulomb criterion (Figure 4.1.b) predicts stable mud weights as high as 1.38-1.4 sg, and the Mogi-Coulomb criterion (Figure 4.1.c) predicts stable mud weights of 1.23 sg. A recent study by Rahimi and Nygaard (2015) has shown that while the Modified Lade is an overly optimistic criterion, and the Mohr-Coulomb criterion being overly conservative, the Mogi-Coulomb criteria yields a more reliable and realistic estimate of the minimum mud weight. For the case of Well A, an increase in mud weight of 0.13 – 0.15 sg would have resulted in a "trouble-free", stable well for the drilled trajectory. As Figure 4.1.c shows, a mud weight of 1.1 sg would have required an azimuth of 141° (parallel to the minimum horizontal stress ordination) and an inclination angle higher than 60°. As can be seen from Table 4.1, all wells in Field E of the Mishrif Formation experiencing wellbore collapse and associated "stuck pipe" (Wells A, E and H) have been drilled with a mud weight less than suggested by the Mogi-Coulomb criterion. It is therefore concluded that the presented 1D MEM approach can be used to mitigate all wellbore collapse problems observed in Field E

For Well B, the operator tried to support the wellbore by increasing the mud weight (1.22 sg; without geomechanical consideration) resulting in high overbalance pressure conditions, which caused differential sticking. The Modified Lade criterion (Figure 4.2.a) suggests that a reduction to 1.09 sg would be possible, however as shown for Well A, this would increase the likelihood of collapse. The Mohr-Coulomb criterion (Figure 4.2.b) even suggests a higher minimum mud weight than used, and therefore cannot be considered. The Mogi-Coulomb criterion would enable a reduction of 0.05 sg before risking the onset of collapse. If this reduction still results in differential sticking, the optimal drilling trajectory (with an azimuth of 141° and an inclination of more than 60°) would enable to use a mud

weight as low as 1.05 sg. As can be seen in Table 4.1, all wells in Field E of the Mishrif Formation experiencing differential sticking (Wells B, C, D, F and G) have been drilled with a mud weight higher than suggested by the Mogi-Coulomb criterion.

5. CONCLUSIONS

This study shows that drilling operations in the Mishrif formation were conducted without considering an appropriate geomechanical analysis. The operating minimum mud weight was assigned based on the interpolated pore pressure distribution, and widespread borehole collapse was observed in several wells in the Mishrif Formation. A simple 1D MEM used to calculate the minimum mud weight (based on the principal stresses of an arbitrary oriented wellbore) shows that the widespread stability problems could have been prevented. The results of this study document the prediction of the minimum mud weight based on three different failure criteria. The results obtained from the Mogi–Coulomb failure criterion, which are chosen as the most indicative failure criterion to assess wellbore collapse (e.g. Rahimi and Nygaard, 2015), indicate that all wells experiencing collapse and associated stuck pipe have been drilled with too low of a mud weight. The 1D MEM approach can be used to design an optimal minimum mud weight for future wells based on the results presented. Based on the horizontal stress orientations, this study recommends well azimuths along the minimum horizontal stress direction with inclinations higher than 40°.

In addition to addressing wellbore collapse, the 1D MEM approach can also be used to mitigate the occurrence of differential sticking as observed for several wells in the Mishrif Formation. The results presented show that all wells experiencing differential sticking have been drilled with a mud weight higher than suggested by the Mogi-Coulomb criterion. It is therefore concluded that adhering to the minimum mud weight predicted by the Mogi-Coulomb failure criterion reduces the likelihood of wellbore collapse and also limits the potential for differential sticking in the E oilfield in the Mishrif Formation.

Table 4.1: Well trajectory data, actual used mud weight, recommended mud weight for the three different failure criteria, and associated geomechanical problems for eight wells in the Mishrif Formation

Well No.	Azi.	Inc.	Actual MW [sg]	Min. MW (Mohr-Coulomb)	Min. MW (Mogi-Coulomb)	Min. MW (Modified Lade)	Drilling Challenge
A	188	38	1.1	1.38	1.23	1.17	Stuck pipe
B	158	19	1.22	1.31	1.17	1.09	Differential sticking
C	228	33	1.22	1.2	1.07	0.98	Differential sticking
D	39	20	1.2	1.36	1.15	1.1	Differential sticking
E	187	40	1.11	1.46	1.31	1.18	Stuck pipe
F	38	31	1.2	1.28	1.14	1.12	Differential sticking
G	279	37	1.1	1.04	0.9	0.82	Differential sticking
H	214	41	1.22	1.62	1.43	1.37	Stuck pipe

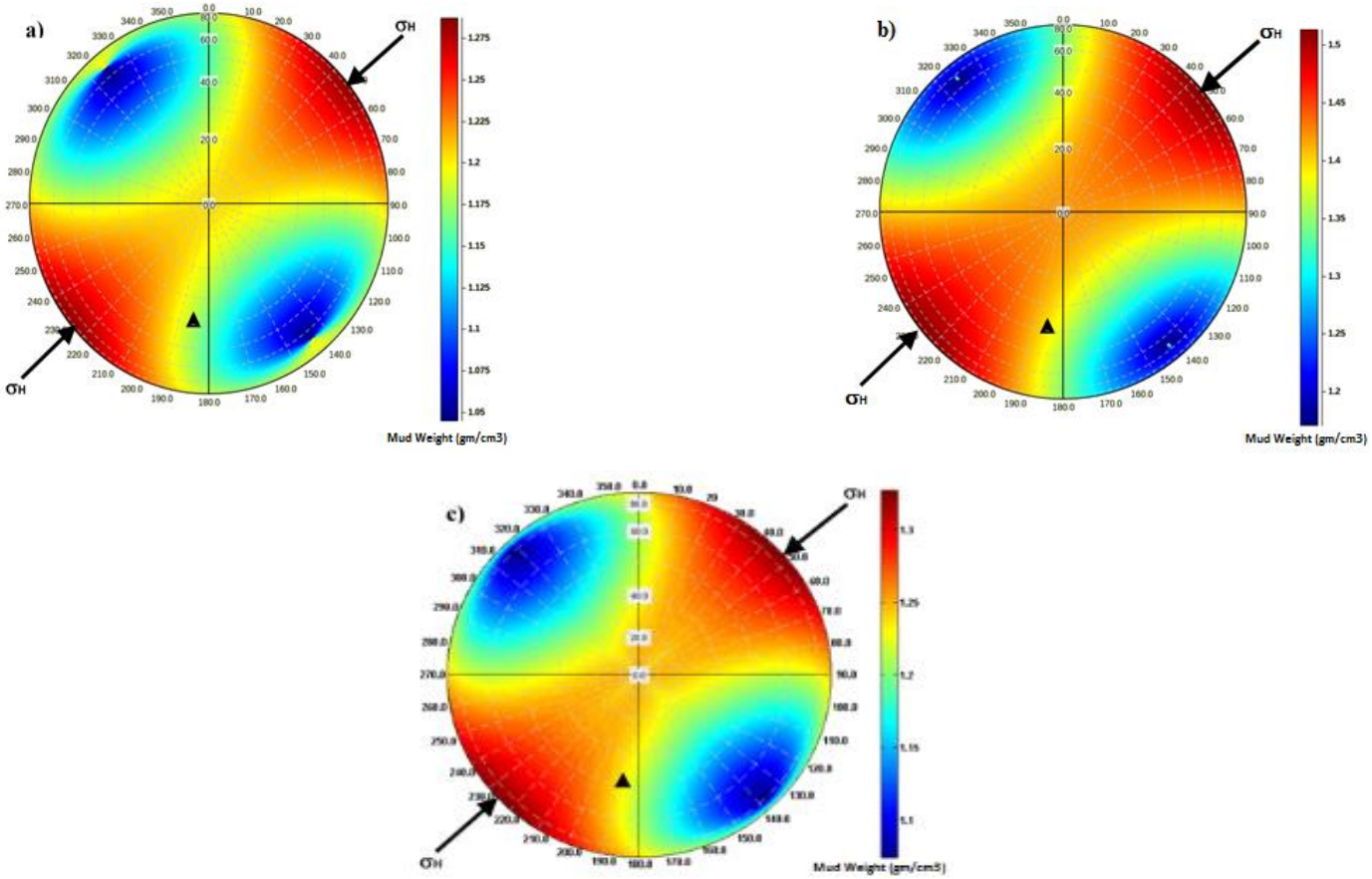

Figure 4.1: Minimum mud weight plots for different failure criteria for Well A. The triangular symbol shows the azimuth and inclination of the actual well (drilled with a mud weight of 1.1 sg) which experienced wellbore collapse. a) Modified Lade failure criterion, b) Mohr-Coulomb failure criterion, c) Mogi-Coulomb failure criterion. In the contour plots, the azimuths (from north 0º to 360º) are labeled around the perimeter; and the well inclination (from vertical 0º to horizontal 90º) are labeled along the radial direction

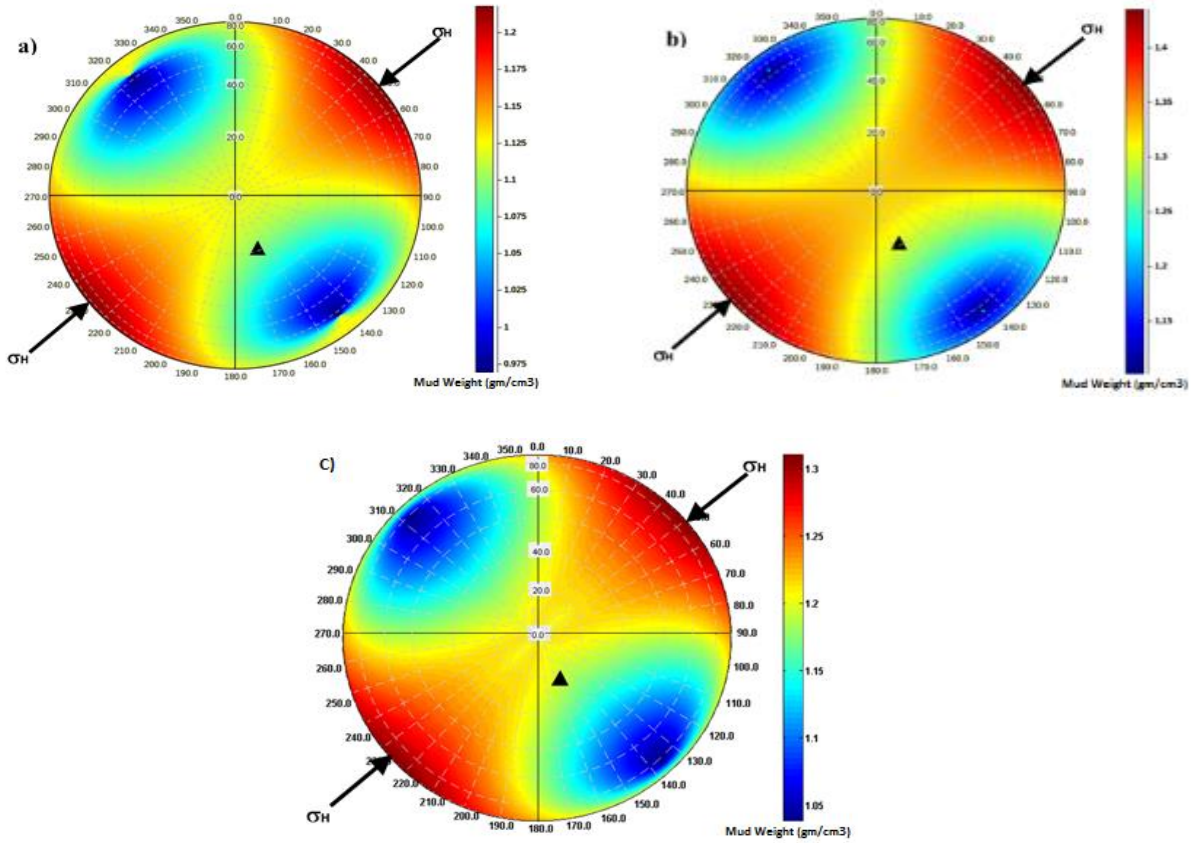

Figure 4.2: Minimum mud weight plots for different failure criteria for Well B. The triangular symbol shows the azimuth and inclination of the actual well (drilled with a mud weight of 1.22 sg) which experienced wellbore collapse. a) Modified Lade failure criterion, b) Mohr-Coulomb failure criterion, c) Mogi-Coulomb failure criterion. In the contour plots, the azimuths (from north 0º to 360º) are labeled around the perimeter; and the well inclination (from vertical 0º to horizontal 90º) are labeled along the radial direction

ABBREVIATIONS

FBP	Formation breakdown pressure
FCP	Fracture closure pressure
FIT	Formation integrity tests
FMI	Formation micro-imager
Int Pp	Interpolated pore pressure
ISIP	Instantaneous shutt-in pressure
LOT	Extended leak-of-test
Max FBP	Maximum formation breakdown pressure
Max Pp	Maximum pore pressure
Min FBP	Minimum formation breakdown pressure
Min Pp	Minimum pore pressure
MEM	Mechanical earth model
MW	Mud weight
MWD	Measuring while drilling
NPHI	Neutron porosity
NPT	Non- productive time
TVD	True vertical depth
UCS	Unconfined compressive strength
V_{shale}	Shale volume

NOMENCLATURE

C_o	Unconfined compressive strength
DTCO	Sonic log
E dyn	Dynamic Young's Modules
E stat.	Static Young's Modules
G	Bulk Modules
i	Inclination
k	Stress path coefficient
NF	Normal Fault
P_o	pore pressure
P_w	Mud Weight
q	flow factor parameter
r	Distance from wellbore
R	Wellbore radius
RHOB	Density log
S_o	Cohesion of the rock
S	Lade cohesion of the rock
T_o	Tensile strength
V_p	Compressional wave
V_s	Shear wave
w_{BO}	Breakout Width
z	Vertical depth
α	Azimuth
$\alpha_{1\,,\,k}$	Drucker-Prager constants
η	Lade internal friction

ρ	Bulk density
σ_h	Minimum horizontal stress
σ_H	Maximum Horizontal Stress
$\sigma_{m,2}$	mean effective stress
σ_{oct}	octahedral stress
σ_{rr} , $\sigma_{\Theta\Theta}$, σ_{zz}	Radial , Tangential and axial stresses
σ_v	Vertical stress
σ_x , σ_y , σ_z	Normal stresses
τ_{oc}	Octahedral shear stress
φ	Internal friction angle

REFERENCES

Al-Ajmi AM, Zimmerman RW. The Relation between the Mogi and the Coulomb failurecriteria. Int J Rock Mech Min Sci 2005; 42 pp 441–439.

Al-Ajmi AM, Zimmerman RW. A new well path optimization model for increased mechanical borehole stability. Journal of Petroleum Science and Engineering 2006; 69 (2009) 53–62.

Aadnoy BS, Looyeh R. Petroleum rock mechanics drilling operations and well design. 1st edition. Oxford: Gulf Professional Pub, 2011.

Aadnoy BS. Stresses around horizontal boreholes drilled in sedimentary rocks. J. Petrol. Sci. Eng. 2, pp 349–360, 1989.

Aqrawi AAM, Goff JC, Horbury AD, Sadooni FN. The petroleum geology of Iraq. 1st edition. Scientilic Press Ltd, 2010.

Azim SA, Mukherjee P, Al-Anezi SA, Al-Otaibi B, Al-Saad B, Perumalla SV, Babbington JF. Using an Integrated Geomechanical Study to Resolve Expensive Wellbore Stability Problems While Drilling Through the Zubair Shale/Sand Sequence of Kuwait: A Case Study. In: SPE/IADC Middle East Drilling and Technology Conference and Exhibition, Muscat, Oman, 24-26 October 2011; doi:10.2118/148049-MS.

Bell JS. Investigating stress regimes in sedimentary basins using information from oil industry wireline logs and drilling records. In Hurst, A., M. Lovell and A. Morton (eds.): Geological applications of wireline logs, Geol. Soc. Lond. Spec. Publ. 1990; 48, pp 305-325.

Bell JS, Babcock EA. The Stress Regime of The Western Canadian Basin and Implications for Hydrocarbon Production. Bulletin of Canadian Petroleum Geology 1986; Vol. 34, No. 3. (September), pp 364-378.

Chang C, Zoback MD, Khaksar A. Empirical relations between rock strength and physical properties in sedimentary rocks, Journal of Petroleum Science and Engineering 2006; Volume 51, Issues 3–4, pp 223-237.

Charlez P. Rock Mechanics. Vol. I. Theoretical Fundamentals, Editions Technip, Paris, 1991.

Ewy RT. Wellbore-Stability Predictions by Use of a Modified Lade Criterion. Society of Petroleum Engineers 1999; doi:10.2118/56862-P.

Fjaer E. Petroleum related rock mechanics. 2nd edition. Amsterdam: Elsevier, 1992.

Gholami R, Maleki S, Moradzadeh A, Rasouli V, Hanachi J. Practical application of failure criteria in determining safe mud weight windows in drilling operations. Jornal of Rock Mechanics and Geotechnical Engineering 2014; 6 (2014) 13-25.

Heidbach, O., Tingay, M., Barth, A., Reinecker, J., Kurfeß, D. and Müller, B., The World Stress Map database release 2008 doi:10.1594/GFZ.WSM.Rel2008, 2008.

Helmick WE, Longley AJ. Pressure-differential Sticking of Drill Pipe and How It Can Be Avoided or Relieved. In: the spring meeting of the Pacific Coast District, Division of Production, Los Angeles, May 1957, pp 55-61.

Jaeger JC, Cook NG, Zimmerman R. Fundamentals of Rock Mechanics. Blackwell, 4th edition, April 2007, Wiley-Blackwell.

Jarosiński M. Contemporary stress field distortion in the Polish part of the Western Outer Carpathians and their basement, Tectonophysics 1998; Volume 297, Issues 1–4, 20 pp 91-119, ISSN 0040-1951.

Jassim SZ, Goff JC. Geology of Iraq. 1st edition. Prague: Dolin, 2006.

Kristiansen TG. Drilling Wellbore Stability in the Compacting and Subsiding Valhall Field: A Case Study. J SPE Drilling and Completion, 2007; pp 277-295, doi:10.2118/87221-PA.

Maleki S, Gholami R, Rasouli V, Moradzadeh A. Comparison of different failure criteria in prediction of safe mud weigh window in drilling practice, Earth-Science Reviews 2014; Volume 136, pp 36-58, ISSN 0012-8252.

Mastin L. Effect of borehole deviation on breakout orientations, J. Geophys. Res. 1988; 93(B8), 9187–9195, doi:10.1029/JB093iB08p09187.

Moos D, Zoback MD. Utilization of observations of well bore failure to constrain the orientation and magnitude of crustal stresses: Application to continental, Deep Sea Drilling Project, and Ocean Drilling Program boreholes, J. Geophys. Res. 1990; 95(B6), 9305–9325, doi:10.1029/JB095iB06p09305.

PešKa P, Zoback MD. Compressive and tensile failure of inclined well bores and determination of in situ-stress and rock strength. Journal of Geophysical Research Atmospheres 1995; 100(B7):12791- · July 1995. DOI: 10.1029/95JB00319.

Plumb RA. Influence of composition and texture on the failure properties of clastic rocks. In: Eurocks 94, rock mechanics in petroleum engineering conference 1994; pp 13–20.

Rahimi R, Nygaard R. Comparison of rock failure criteria in predicting borehole shear failure. International Journal of Rock Mechanics & Mining Sciences 2015; 79(2015)29–40.

Rehm B, Schubert J, Haghshenas A, Paknejad A, Hughes J. Managed Pressure Drilling. 1st edition. Gulf Publishing Company, Houston, 2008.

Schroeter DR, Chan HW. Successful Application of Drilling Technology Extends Directional Capability. J SPE Drilling Engineers 1989; doi:10.2118/17660-PA.

Sibley MJ, Bent JV, Davis DW. Reservoir Modeling and Simulation of a Middle Eastern Carbonate Reservoir. Society of Petroleum Engineers 1997; doi:10.2118/36540-PA.

Stewart G, Wittmann M. Interpretation of The Pressure Response Of The Repeat Formation Tester. Society of Petroleum Engineers 1979; pp 230-236, doi:10.2118/8362-MS.

Tingay M, Bentham P, De Feyter A, Kellner A. Present-day stress field rotations associated with evaporites in the offshore Nile Delt. Geological Society of America Bulletin 2011; 123(5-6):1171-1180 · May 2011.DOI: 10.1130/B30185.1.

Torres ME, Gonzalez AJ, Last NC. In-Situ Stress State Eastern Cordillera (Colombia). In: SPE Latin American and Caribbean Petroleum Engineering Conference held in Port-of-Spain, Trinidad, West Indies, 27–30 April 2003; doi:10.2118/81074-MS.

Zajac BJ, Stock JM. Using Borehole Breakouts to Constrain the Complete Stress Tensor: Results from the Sijan Deep Drilling Project and Offshore Santa Maria Basin California. - J. Geophys. Res. 1992; 102, pp 10083-10100.

Zoback ML. First and second order patterns of tectonic stress: The World Stress Map Project. Journal of Geophysical Research 1992; 97, pp 11,703–11,728.

Zoback MD. Reservoir Geomechanics. 1st edition. Cambridge: Cambridge University Press, 2010.

Zoback MD, Barton CA, Brudy M, Castillo DA, Finkbeiner T, Grollimund BR, Moos DB, Peska P, Ward CD, Wiprut DJ. Determination of stress orientation and magnitude in deep wells. International Journal of Rock Mechanics & Mining Sciences 2003; 40 (2003) 1049–1076.

Zoback MD, Mastin L, Barton CA. In-situ Stress Measurements In Deep Boreholes Using Hydraulic Fracturing, Wellbore Breakouts, And Stonely Wave Polarization. International Society for Rock Mechanics, 1986.

Zoback MD, Moos D, Mastin LG, Anderson RN. Well bore breakouts and in situ stress. - J. Geophys. Res. 1985; 90, pp 5523-5530.

Zoback MD, Peska P. In-Situ Stress and Rock Strength in the GBRN/DOE Pathfinder Well, South Eugene Island, Gulf of Mexico. Journal of Petroleum Technology 1995; pp 582-585 doi:10.2118/29233-PA.

APPENDIX A

MISHRIF FORMATION LOG DATA

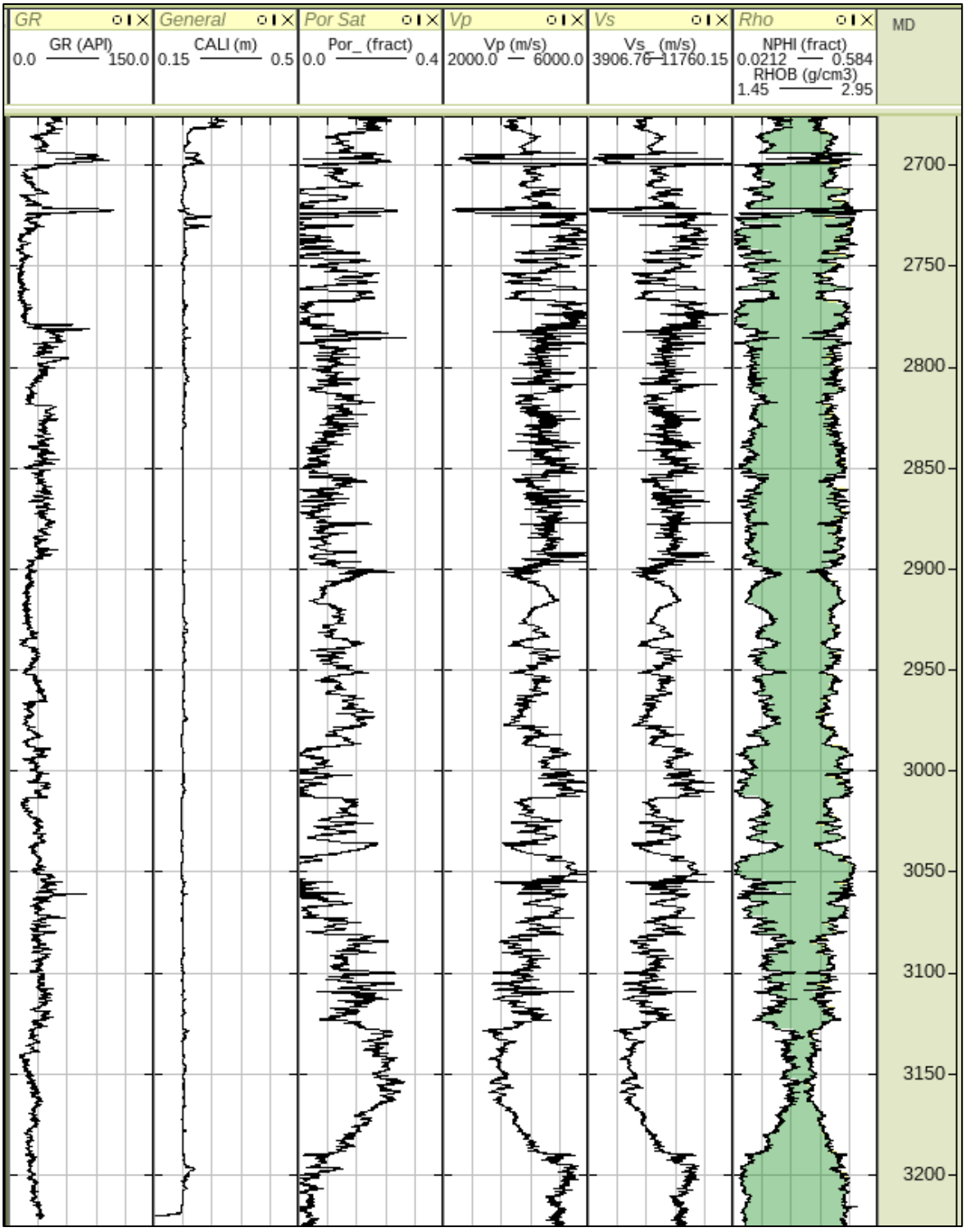
GR
GR (API)
0.0
150.0
General
CALI (m)
0.15
0.5
Por Sat
Por_ (fract)
0.0
0.4
Vp
Vp (m/s)
2000.0
6000.0
Vs
Vs_ (m/s)
3906.76
11760.15
Rho
NPHI (fract)
0.0212
0.584
RHOB (g/cm3)
1.45
2.95
MD
2700
2750
2800
2850
2900
2950
3000
3050
3100
3150
3200

APPENDIX B

QUALITY RANKING SYSTEM

	A	B	C	D
Earthquake focal mechanisms	Average P-axis or formal inversion of four or more single-event solutions in close geographic proximity(at least one event M≥ 4.0, other events M≥ 3.0)	Well-constrained single-event solution (M≥ 4.5) or average of two well-constrained single-event solutions (M≥ 3.5) determined from first motions and other methods (e.g. moment tensor wave-form modeling, or inversion)	Single-event solution (constrained by first motions only, often based on author'squality assignment)(M≥ 2.5). Average of several well-constrained composites (M≥ 2.0)	Single composite solution. Poorly constrained single-event solution. Single-event solution for M < 2.5 event
Wellbore breakouts	Ten or more distinct breakout zones in a single well with sd ≤ 12◦ and/or combined length >300 m. Average of breakouts in two or more wells in close geographic proximity with combined length >300 m and sd ≤ 12◦	At least six distinct breakout zones in a single well with sd ≤ 20◦ and/or combined length > 100 m	At least four distinct breakouts with sd < 25◦ and/or combined length > 30 m.	Less than four consistently oriented breakout or >30 m combined length in a single well. Breakouts in a single well with sd ≥ 25◦.
Drilling-induced tensile fractures	Tenor more distinct tensile fractures in a single well with sd ≤ 12◦ and encompassing a vertical depth of 300 m, or more	At least six distinct tensile fractures in a single well with sd ≤ 20◦ and encompassing a combined length > 100 m	At least four distinct tensile fractures with sd < 25◦ and encompassing a combined length > 30 m.	Less than four consistently oriented tensile fractures with <30 m combined length in a single well. Tensile fracture orientations in a single well with sd ≥ 25◦.
Hydraulic fractures	Four or more hydrostatic orientations in a single well with sd ≤ 12◦ depth >300 m. Average of hydrofrac orientations for two or more wells in close geographic proximity, sd ≤ 12◦	Three or more hydrofrac orientations in a single well with sd < 20◦. Hydrofrac orientations in a single well with 20◦ < sd < 25◦	Hydrofac orientations in a single well with 20◦ < sd < 25◦. Distinct hydrofrac orientation change with depth, deepest measurements assumed valid. One or two hydrofrac orientations in a single well.	Single hydrofrac measurements at <100 m depth.

II. A NEW DRIVER FOR MANAGED PRESSURE DRILLING: REDUCING STUCK PIPE OCCURRENCE

ABSTRACT

Differences between higher mud pressure in a wellbore and lower pore pressure in high permeability rocks can lead to differential sticking, particularly when drilling deviated wells and encountering mud losses. Several solutions, all challenging, can be utilized to address this problem. The conventional mitigation has been to manage mud weight accordingly. However, managed pressure drilling (MPD) offers a promising solution with positive risk-adjusted cost and other benefits perspective.

Wells in the E oilfield in southern Iraq are typically drilled overbalanced and therefore often experience a high percentage of non-productive time (NPT) due to differential sticking. This study evaluates the feasibility of using MPD to optimize the drilling process by decreasing mud weight while applying required surface pressure to achieve the target bottom hole pressure (BHP). DZxION CSM software simulation uses different mud weights to determine required choke surface backpressure (SBP) to achieve the initial target equivalent circulation density (ECD).

Historically, differential sticking has not been a primary driver to justify MPD. However, MPD offers more dynamic and rapid wellbore pressure control by adjusting SBP applied to the annulus for a given mud weight (MW), and can actually decrease the risk of differential sticking. Instead of shifting MW or changing other drilling parameters, MPD adjusts the required ECD and/or equivalent static density (ESD) based on the formation pore pressure gradient. Additionally, in the event of mud losses due to high ECD/ESD, MPD directly lowers SBP to decrease the BHP without the need to reduce MW.

This paper discusses hydraulic simulation software used to model the drilling development plan. The software optimizes MPD parameters including MW and SBP while drilling, making pipe connections, and completing the well. Furthermore, it discusses the sensitivity effects of each parameter on wellbore pressure and provides guidelines for managing pressure by adjusting these variables.

1. INTRODUCTION

The E onshore oilfield is located in southern Iraq and is considered one of the giant oil and gas fields in the Middle-East with more than thirteen carbonate and sandstone reservoirs. The two main reservoirs are the Mishrif formation and the Zubair formation with different equivalent pore pressures of 4.165 ppge and 9.5 ppge, respectively. The operator planned to drill both formations in the same hole (8 ½" section) to reduce the drilling cost. However, this plan led to a high percentage of non- productive time (NPT) due to wellbore instability. NPT is time associated with kicks, wellbore breathing, lost mud, lost circulation materials, additional casing string(s), stuck pipe, unplanned sidetracks and in some cases not reaching total depth (TD).

One of the most significant drilling operation challenges in this field was differential sticking in the Mishrif formation, which has the minimum pore pressure in this hole section, compounded by the high mud weight required to keep the BHP higher than the pore pressure exposed in other formations in this hole. Differential sticking can result when pressure from an overbalanced mud column acts on the surface area of the drill string against a filter cake deposited across a permeable formation. The surface area of the pipe that is embedded into the mud cake has a pressure equal to the pore pressure acting in one direction while the hydrostatic pressure acts in the other direction. When the hydrostatic pressure in the wellbore is higher than the formation pressure, the pressure difference forces the pipe towards the borehole wall. This usually occurs along the drill collars because there is less annular clearance to begin with the drill collars usually have larger diameter, which increases the crossectional area that is in contact with the borehole, and

the drill collars are the first section of the pipe to encounter the permeable formation (Rehm and et al., 2008).

This study investigates using leading technology, either under balance drilling (UBD) or MPD, to optimize the drilling process in an 8 1/2" hole by using the lowest reasonable mud weight. MPD also may require the application of the required pressure at the surface. The modern drilling technology parameters will be adjusted based on the formation pore pressure. SBP can be manipulated according to the newly exposed formation's pore pressure, and if required, the mud weight can be changed to give more flexibility to cope with a rapid change in pore pressure regime. Hydraulic simulations are run with different mud weights to determine the optimum back pressure to achieve the initial target ECD at the top of the pressure window.

2. MPD OR UBD

The MPD/UBD candidate selection process is based on two crucial points. The first is the intended method for handling any influx. The second is a formation geomechanical assessment is made to determine the probable wellbore stability pressures, pore pressures and fracture pressures for the candidate hole section (Malloy & Shayegi, 2010). In oilfield E, the objective is to mitigate drilling problems (i.e., stuck pipe) with the added stipulation of preventing influx during the drilling operation.

MPD is used primarily to resolve drilling hazards, although some reservoir benefits can be achieved. MPD offers a reduction in the degree of overbalance, and thus, the impact of drilling fluid on virgin formations will usually decrease, resulting in some reservoir benefits. While UBD can address the same issues (except wellbore instability) and can gain reservoir benefits like minimizing formation damage and early production recovery while drilling, it may not be necessary to go underbalanced to solve the drilling problems in many cases.

The equipment requirements for both UBD and MPD operations are similar; however, there are variations depending on the design parameters of the project. In some instances, the same equipment setup is necessary for both the UBD and MPD methods. The distinguishing difference is that fluid influx is not expected during drilling for an MPD setup. In this study, MPD was selected as more efficient and economically feasible than UBD because wellbore instability is an issue, and MPD is meant to preclude influx from the formation during the drilling operation.

3. MPD STRATEGY TO REDUCE STUCK PIPE RISK

The MPD can enhance drilling practice and prevent stuck pipe by applying many approaches (Rehm 2008). First of all, MPD reduces the overbalance pressure against any formation, minimizing differential pressure and reducing the possibility of stuck pipe occurrence, while gaining some reservoir benefits. Second, the constant bottom hole pressure (CBHP) technique provides the ability to maintain the same pressure on the wellbore constant during drilling, connection, and tripping in or out of the hole. This reduces cycling of the pressure on the wellbore and hence reduces the risk of stuck pipe. Third, an MPD system with PLC automatic control provides the possibility to exert and relieve pressure on the wellbore as required to increase or decrease the ECD nearly instantly (Hannegan 2011). This can be done by manipulating the MPD choke manifold at the surface, and this provides the ability to manipulate the ECD as required to get the string un-stuck within minutes. Fourth, the control system has been improved by using intelligent techniques such as smart instrumentation with real-time diagnostics, large diaphragm seals transducers, multi-sensor voting systems, auto tracking pressure relief valve control, and adaptive self-tuning surface back pressure (SBP) control (Moosavinia et al. 2016). Finally, MPD can directly affect a project's financial viability and improve safety by reducing mud weight and NPT, and improving precise pressure control.

4. METHODOLOGY

CBHP was recognized as a suitable method of MPD to minimize the overbalanced mud weight while applying surface backpressure to avoid differential sticking. CSM software was used to perform offline hydraulic analysis and calculations. This software was developed by Sagar Nauduri while at Texas A&M University, to test the suitability of the formation to be drilled using MPD.

4.1 SOFTWARE INPUT DATA

DZxION MPD CSM software calculates the annular and pipe pressure drop based on the API RP 13D rheological model. For this software, the essential input parameters are as follows:

Wellbore Schematic	Geomechanical data
➢ Casing shoe depth	➢ Pore pressure gradient
➢ Target depth	➢ Fracture pressure gradient
➢ Hole size	➢ Formation collapse gradient
➢ Casing size	Bottom Hole Assembly
➢ Water depth	➢ String size (OD & ID)
Well geometry	➢ String length
➢ Measured depth (MD)	➢ Bit size
➢ Deviation	Drilling Fluid
➢ Azimuth	➢ Drilling fluid properties

4.2 DZXION MPD CSM APPROACH

The software calculates ECD based on the input data and compares it with the formation pressures window to determine whether this ECD is acceptable or not. If the hydraulic and the circulating pressures in the openhole section of the well are between the

pore pressure and fracture pressures, the well does not need the MPD. If these pressures are below the pore pressure or exceeds the fracture pressure, the software offers a different mud weight and SBP. Then, the software decides if MPD is applicable or not (Nauduri & Medley 2010).

5. RESULTS AND DISCUSSION

In the E oilfield, after running and cementing 9 5/8 " casing to 8,769 ft. drilling continues with an 8 ½ " bit without major kick or loss problems according to the planned mud weight. After drilling the cement, the operator changes the MW from 11 ppg to 10.1 ppg because the pore pressure expected in the Mishrif formation is lower than the pore pressure in the previous hole. Furthermore, as noted above, keeping the mud weight at a minimum value reduces the differential pressure between the mud pressure and pore pressure to avoid the stuck pipe. Drilling continues to the planned 7" casing setting depth at 13,740ft. To keep the well under control in the Zubair formation, the operator increases the mud weight to 12 ppg.

Simulations of many cases and conditions were conducted using the software which is presented in Tables 5.1, 5.2, 5.3, 5.4 and 5.5.

5.1 CONVENTIONAL DRILLING

The simulator shows the drilling MW must be maintained between 12 ppg and 12.3 ppg with more than 700 gpm flow rate in order to drill conventionally, as a shown in Figure 5.1. Otherwise, there is a high probability for kick or fluid loss occurrence. However, this MW generates a large differential pressure across the Mishrif formation that leads to differential sticking. These results demonstrate that lower mud weight is inevitably required while compensating the BHP by applying SBP with a choke and back pressure pump.

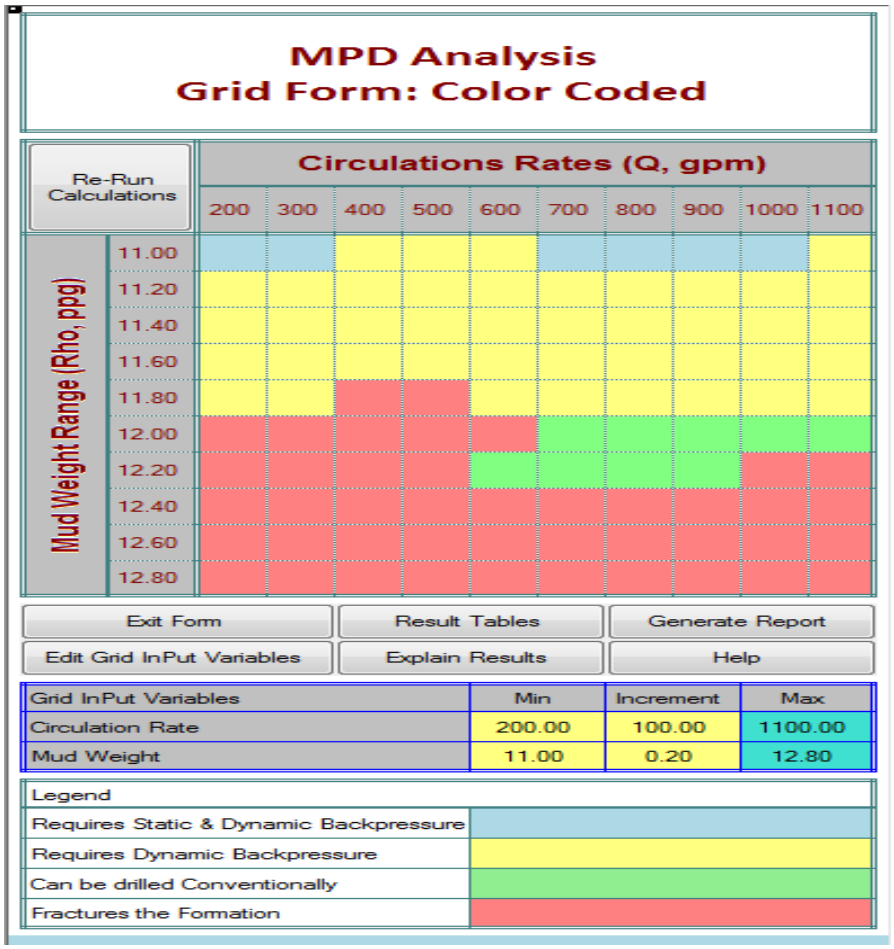

Figure 5.1: The conventional drilling analysis in CSM simulator

Table 5.1: Hole section geomechanical information

Formation	TVD (ft.)	PP (lower limit) (ppg)	FP (lower limit) (ppg)
Upper Faris	59	8.33	13.82
Lower Faris	2980	8.33	14.16
Ghar	3955	8.33	13.82
Dammam	4385	8.33	13.82
Um-Rudhoma	4964	8.33	13.82
Tayrat	6047	8.33	13.91
Shiransh	6400	8.33	14
Hartha	6809	7.66	14.30
Saadi	7219	9.7	14.30
Tanuma	7544	9.8	14.24
Khasib	7685	9.9	14.24
Mishrif	7849	4.16	14.16
Rumila	8646	9.3	14.16
Ahmdi	8698	9.4	13.80
Mauddud	9229	9.3	13.80
Nahr Umr	9777	9.3	13.80
Nahr Umr Sand	10217	9	12.50
Shuaiba	10397	8	12.50
Zubair	10942	9.5	13.80
Ratawi	12300	9.3	13.80

.

Table 5.2: J-shape and S-shape well geometry

S-Shape			J-Shape		
Measured Depth (ft.)	Inclination (^{o})	Azimuth (^{o})	Measured Depth (ft.)	Inclination (^{o})	Azimuth (^{o})
0	0	0	0	0	0
675	0.26	119.39	370	0.07	114.22
1138	0.15	104.1	1243	0.17	295.22
1613	0.14	19.89	1904	0.1	181.16
1984	0.6	100.57	2385	0.14	37.43
2460	12.41	7.36	2587	0.93	188.33
2939	21.53	5.3	3608	23.7	184.79
3414	32.23	7.46	3796	29.23	187.02
3789	35.61	6.6	4368	29.77	191.03
3884	36.75	6.73	5231	36.03	188.28
4360	35.09	5.33	5805	41.07	188.56
5495	29.88	6.56	6851	39.76	184.76
5971	31.32	4.02	7235	39.34	185.29
6444	31.85	4.44	7521	38.31	185.24
6921	32.94	3.78	7712	37.72	185.58
7393	30.68	2.49	8092	36.55	186.05
7867	29.82	3.97	8721	31.58	187.3
8340	28.47	6.49	9759	40.48	186.2
8818	25.95	6.33	10624	41.83	186.72
9284	25.79	9.88	10706	40.43	186.33
9759	26.66	10.9	10994	40.83	187.03
10237	20.9	6.24	11566	40.15	189.4
10756	9.24	3.86	11947	34.1	190.41
11232	1.02	299.66	12232	30.92	190.53
11708	1.97	287.03	12709	29.14	192.21
12181	1.9	3.12	12792	28.6	191.67
12654	2.86	2.81	12868	28.6	191.67
13086	4.33	280.61	13456	17.49	210.68
13224	4.76	282.23	13745	13.33	215.98

Table 5.3: Two casing designs information

Casing	First Casing Design					Second Casing Design				
	Bit size	Casing		Depth (1000ft.)		Hole	Casing		Depth (1000ft.)	
		OD	ID	From	To	Diameter	OD	ID	From	To
Liner	8 ½"	7"	6 ½"	8.7	13.7	6 3/4"	5 1/2 "	4 7/8"	8.7	13.7
Production	12 ¼"	9 5/8"	8 5/8"	0	8.7	12 ¼"	9 5/8"	8 5/8"	0	8.7
Intermediate	16"	13 3/8"	12 3/8"	0	4.6	16"	13 3/8"	12 3/8"	0	4.6
Surface	26"	18 5/8"	17 5/8"	0	2.5	26"	18 5/8"	17 5/8"	0	2.5
Conductor	36"	30"	28 ¾"	0	3.3	36"	30"	28 ¾"	0	3.3

Table 5.4: Two BHA designs

Item Description	Frist BHA Design			Second BHA Design		
	ID (in)	OD (in)	Length (ft.)	ID (in)	OD (in)	Length (ft.)
PDC bit	3.5	8	1.15	3.5	6	1.15
8" Sperry Drill Lobe	5.25	8	29.06	5.25	6	29.06
11-3/4" Integral Blade	3	8	7.61	3	6	7.61
8" Float Sub	3	8	2.98	3	6	2.98
8" HOC	3.25	8.08	32.27	3.25	6.08	32.27
8" Downhole screen	3	8.03	7.71	3	6.03	7.71
Circulation sub.	3.5	8.25	8.92	3.5	6.25	8.92
Drill collar	2.813	8.25	92.40	2.813	5.125	92.40
Jar	2.75	8.12	21.88	2.75	5.25	21.88
Drilla collar	2.813	8.25	61.80	2.813	5.25	61.80
X-over Sub.	3	6.75	3.87	2 11/16	3.5	…..
HWDP	3	5	646.16	2 1/4	3.5	646.16
Drill pipe	4.276	5	….	2 11/16	3.5	….

Table 5.5: Ten designs for mud rheology

Rotational Speeds	Fan Viscometer Readings									
	Mud 1	Mud 2	Mud 3	Mud 4	Mud 5	Mud 6	Mud 7	Mud 8	Mud 9	Mud 10
R3	21	21	21	21	19	21	22	25	30	30
R6	29	30	30	30	30	30	31	30	35	35
R100	30	30	30	30	30	30	32	35	35	35
R200	36	36	36	36	36	36	38	40	45	45
R300	45	40	40	41	41	50	40	50	50	55
R600	60	50	51	53	57	75	70	80	75	80

5.2 MPD CBHP SOLUTION

In this analysis, many mud weights were considered to drill this section, ranging from 9.6 ppg to 9.9 ppg. Each scenario results in a different SBP and dynamic back pressure (DBP) required to keep the well under control. The results are shown in Figures . 5.2 and 5.3. Figure 5.2 shows the DBP at any flow rate that is required to stay within the acceptable pressure window for different mud weights. Figure 5.3 shows the SBP required while the well is static for any mud weight between 9.6 ppg and 9.9 ppg.

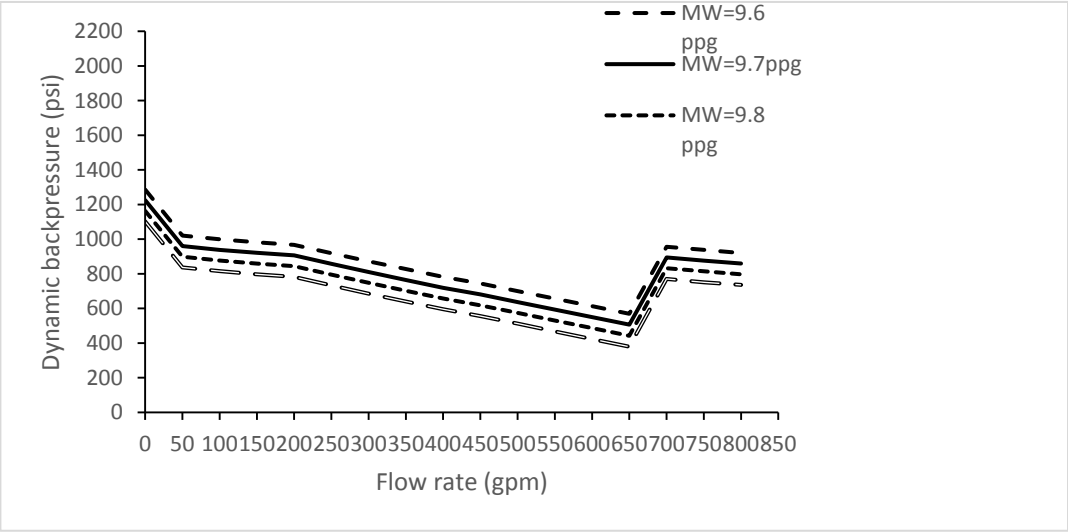

Figure 5.2: The required dynamic back pressure by choke vs. flow rate

5.3 MPD PARAMETER ANALYSIS

During MPD planning the effect of each parameter should be considered to minimize the amount of required back pressure required and to have a more controllable MPD system. Operating pressure window, well geometry, casing design, drill string design and mud rheology are all considered to be MPD parameters, but not all of them are controllable. Furthermore, each one has a different effect on MPD system design.

5.3.1 Operating Pressure Window. The operating window is defined as a lower limit (pore pressure or wellbore collapse pressure) and an upper limit (fracture pressure or leak-off pressure), and is not considered a controllable parameter in the MPD system.

5.3.2 Well Geometry. The wellbore trajectory has a significant impact on MPD according to the difference between hydrodynamic friction and hydrostatic pressure head (Tian and et al. 2007). In this study, two well profiles that are commonly used in the E field (J-shape and S-shape) were compared. The results demonstrate the J-shape profile is recommended over the S-shape because lower choke back pressure is needed to keep the well under control at different flow rates, as a shown in Figures 5.4 and 5.5. Figure 5.4 shows required DBP vs. circulation rate for each trajectory shape. Figure 5.5 shows static SBP vs. MW for each trajectory shape.

5.3.3 Casing And Drill String Design. The hole size and drill string configuration impact all other parameters because the annular clearance can either increase or decrease the friction of the fluid flowing through the annulus. This study compared the current casing and BHA design in this field with other proposed design, as described in Tables 5.3 and 5.4. The results show the current design requires lower dynamic backpressure, as

illustrated in Figure 5.6. Figure 5.6 shows required DBP for various circulation rates for a 7 inch liner design and a 5½ inch liner design.

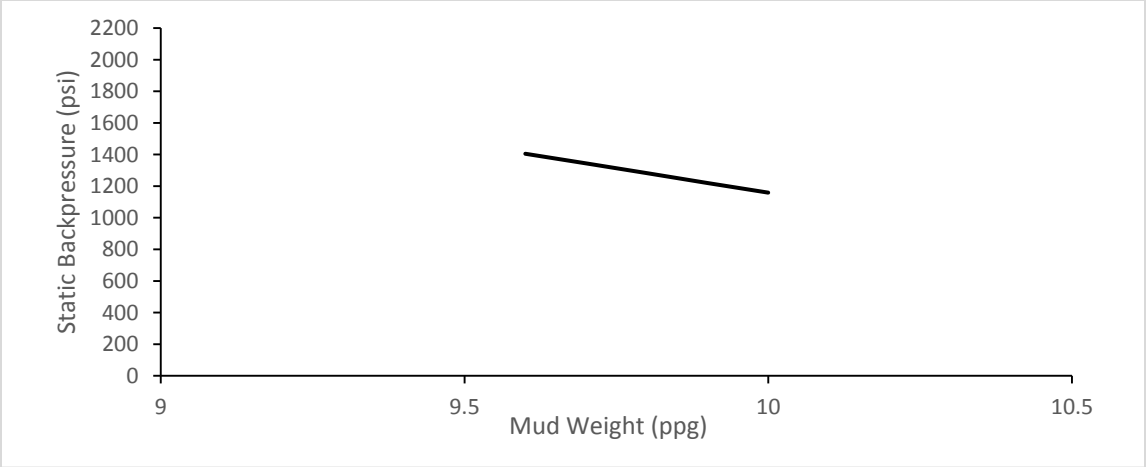

Figure 5.3:The required static back pressure by choke vs. MW

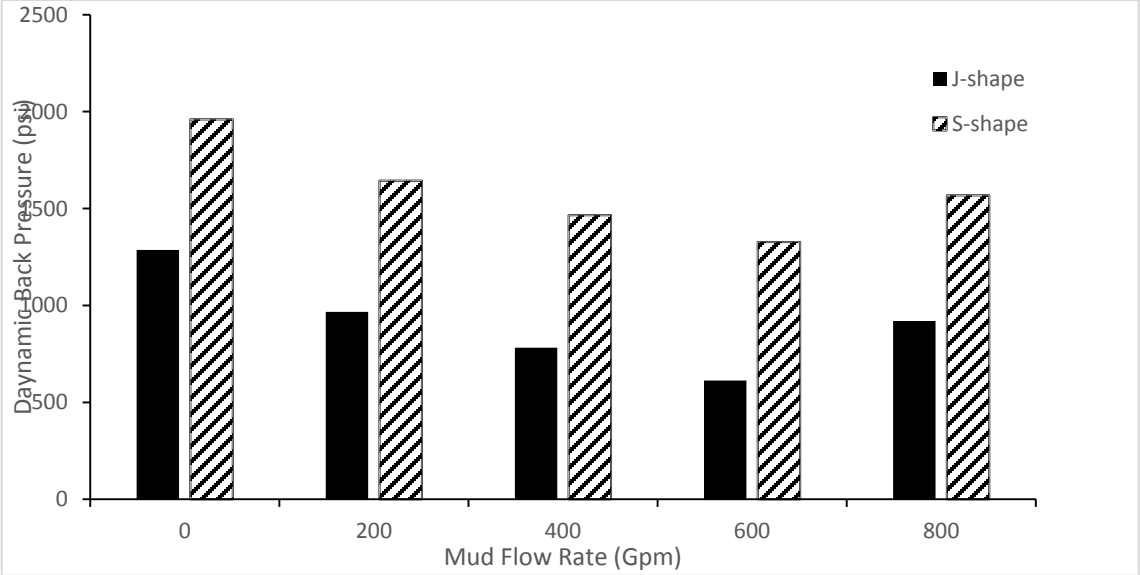

Figure 5.4: The required dynamic choke back pressure vs. flow rate

5.3.3 Casing And Drill String Design. The hole size and drill string configuration impact all other parameters because the annular clearance can either increase or decrease the friction of the fluid flowing through the annulus. This study compared the current casing and BHA design in this field with other proposed design, as described in Tables 5.3 and 5.4. The results show the current design requires lower dynamic backpressure, as illustrated in Figure 5.6. Figure 5.6 shows required DBP for various circulation rates for a 7 inch liner design and a 5½ inch liner design.

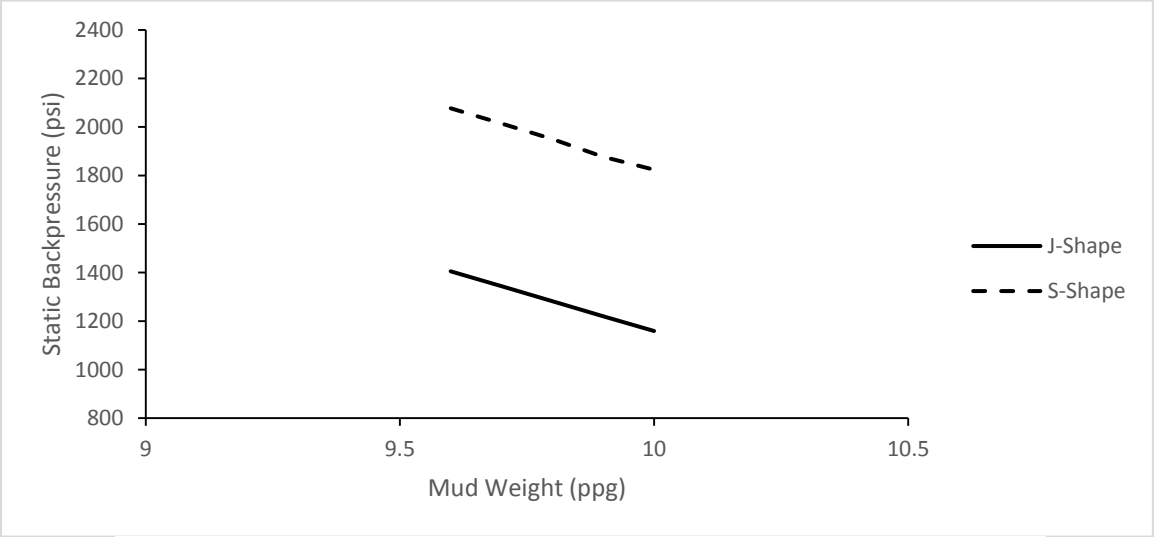

Figure 5.5: The required static back pressure by choke vs. MW

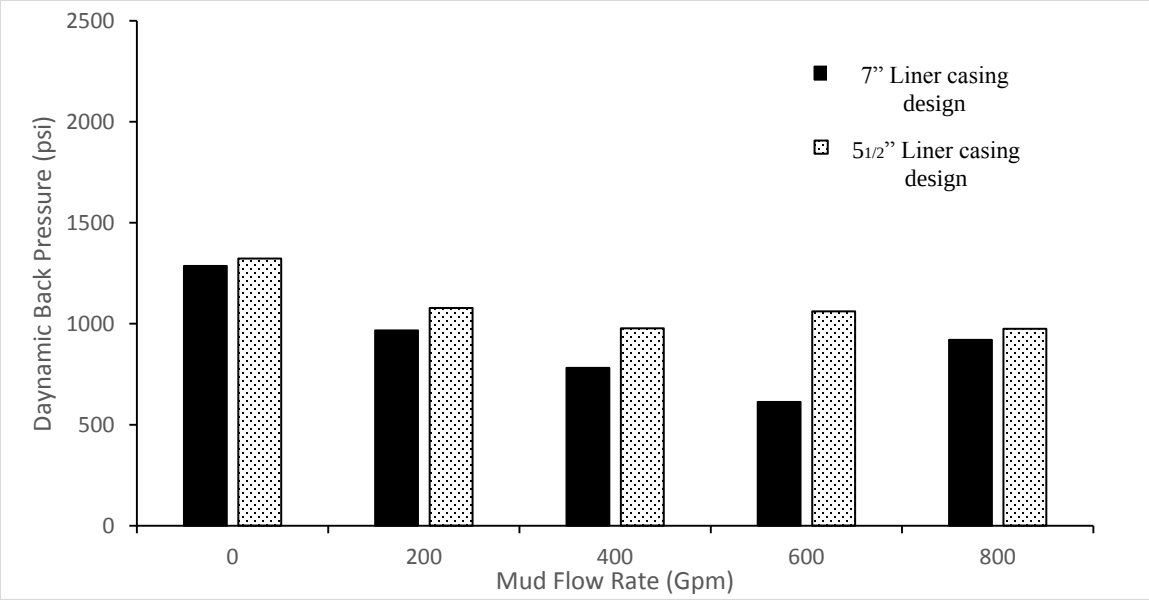

Figure 5.6: The required dynamic back pressure by choke vs. flow rate

5.3.4 Mud Rheology. Rheological properties of drilling fluids play a significant role in managing wellbore pressure. Drilling mud currently used in the field has a non-zero yield point (YP). A non-zero YP causes a sudden pressure jump when the fluid starts to move (pressure increase) or when the fluid is about to stop moving (pressure decrease) (Tian et al. 2007). In this study, ten mud designs were obtained from many drilled wells in this field as a shown in Table 5.5. By simulating these designs and comparing them with each other, mud design No.5 gives the lowest required backpressure as shown in Figure 5.7. Figure 5.7 shows the minimum DBP for each mud required to remain within the pressure window.

Recommendations can be made for oilfield E based on the MPD analysis of different drilling parameters to evaluate their effect on the MPD system performance using the DZxION MPD CSM software. For example, with flowrate equal to 600 gpm and mud weight equal to 9.6 ppg, the best plan includes the following : use of the first BHA (from

Table 5.4), a J-shape trajectory, 7” liner casing design, mud rheology No. 5 from Table 5.5, and 612 psi SBP. Under the same conditions, the worst scenario is the following: the second BHA, an S-shape trajectory, 5.5” liner casing design, and mud rheology No. 9 or 10, which requires 1,830 psi SBP.

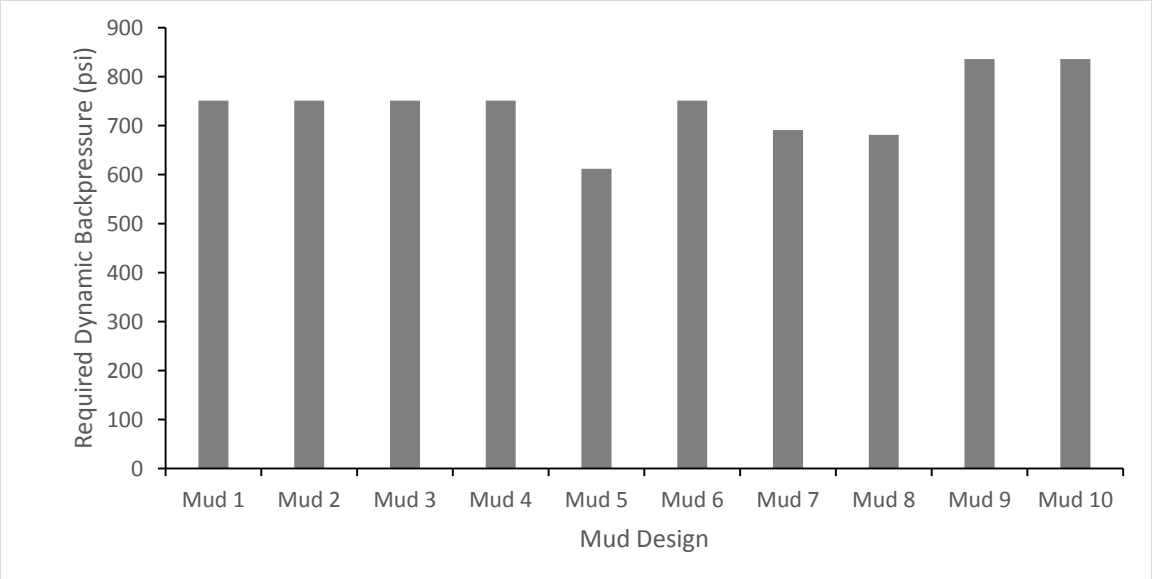

Figure 5.7: The required dynamic back pressure by choke vs. Mud design

6. CONCLUSION

The simulation shows that field is an MPD candidate and introduces SBP to minimize other drilling parameter adjustments and mitigate the stuck pipe problem. The software provides the user with the ability to self-optimize BHA, pump rate, mud properties, well geometry, and required SBP to maintain a stable wellbore. Based on the geomechanical assessment, the drilling hazards (e.g., stuck pipe, kicks and mud losses) can be avoided by compensating the ECD/ESD effects using an MPD approach. Finally, MPD enables drilling a hole section exposing different formation pore pressures in a safe, efficient, and economical way. MPD reduces the operation cost by reducing the NPT and managing mud properties due to the flexibility afforded by adjusting SBP to maintain constant bottom hole pressure for the drilled section.

REFERENCES

Bill Rehm, Jerome Schubert, Arash Haghshenas, Amir Paknejad, Jim Hughes, 2008. Managed Pressure Drilling, Gulf Publishing Company, Houston.

Hannegan, D. 2011. MPD - Drilling Optimization Technology, Risk Management Tool, or Both?. SPE Annual Technical Conference and Exhibition, location, Denver, Colorado, USA, 30 October–2 November. SPE-146644-MS.

Malloy, K. and Shayegi, S. 2010. UBD or MPD: An Engineering Choice Based on Intent. SPE/IADC Managed Pressure Drilling and Underbalanced OperationsConference and Exhibition, Kuala Lumpur, Malaysia, 24–25 February. SPE-173823-MS.

Moosavinia, M. and et al. 2016. Intelligent Control for MPD. SPE/IADC Managed Pressure Drilling and Underbalanced Operations Conference and Exhibition, Galveston, Texas, USA, 12–13 April. SPE-180069-MS.

Nauduri, S. and Medley, G. 2010. MPD Candidate Identification: To MPD or Not To MPD. SPE/IADC Managed Pressure Drilling and Underbalanced Operations Conference and Exhibition, Kuala Lumpur, Malaysia, 24–25 February. SPE-130330-MS.

Tian, S. and et al. 2007. Parametric Analysis of MPD Hydraulics. IADC/SPE Managed Pressure Drilling and Underbalanced Operations Conference and Exhibition, Galveston, Texas, 28–29 March. SPE-108354-MS.

SECTION

2. RECOMMENDATIONS

Although the current study provides useful solutions for wellbore instability problems, many uncertainties and questions are remain unanswered in this work. Below are few recommendations for potential future research opportunities to yield a better solution for this problem:

1. The geomechanical formation properties should be obtained under the true-triaxial core measurements for various facies of the field.
2. The obtained laboratory geomechanical parameters should be correlated to the petrophysical parameters to derive these geomechanical parameters from well logs and to reduce costly geomechanical laboratory measurements in the life cycle of the field.
3. Integrating the Geomechanical results with MPD to prevent the wellbore instability.
4. Annular pressure gauges should be included in the drilling BHA to facilitate the evaluation of the circulation, surge, and pressures.

VITA

Husam Raad Abbood was born in August, 1986, in Basrah, Iraq. He received his bachelor degree in the Fuel and Energy Engineering from Technical College, Basrah, Iraq in 2008; he was among the top three out of 61 students graduated from Fuel and Energy Engineering department in 2008 with a cumulative average of 80.38 %. After graduation, Husam joined the south oil company (S.O.C.) as a drilling engineer. In 2014, he was awarded Scholarship by The Higher Committee for Education Development in Iraq to study for Master's degree in Petroleum Engineering. He started at Missouri University of Science and Technology during the spring semester of 2015 to work under the supervision of Dr. Ralph Flori. He received Master of Science degree in Petroleum Engineering from Missouri University of Science and Technology in December 2016 with 3.806 GPA.